N.T.

CONTRACT NO. NAS8-11181
REQUEST NO. DCN 1-6-53-01162
REPORT NO. GDC DDG 67-006

THE STABILITY OF ECCENTRICALLY STIFFENED CIRCULAR CYLINDERS

VOLUME VI

INTERACTION BEHAVIOR

GENERAL DYNAMICS
Convair Division

REPORT NO. GDC-DDG-67-006

THE STABILITY OF ECCENTRICALLY STIFFENED CIRCULAR CYLINDERS

VOLUME VI

INTERACTION BEHAVIOR

Prepared for the
GEORGE C. MARSHALL SPACE FLIGHT CENTER
National Aeronautics and Space Administration
Huntsville, Alabama

By
G. W. SMITH, E. E. SPIER,
S. N. DHARMARAJAN, and L. S. FOSSUM
20 June 1967

Prepared by
CONVAIR DIVISION OF GENERAL DYNAMICS
San Diego, California

ACKNOWLEDGEMENTS

This volume was prepared by the Structural Analysis Group of General Dynamics Convair Division to present a portion of the results obtained under NASA Contract NAS8-11181. The overall project was conducted in two separate, consecutive phases. The first phase was performed by G. W. Smith and F. A. Dittoe with Dr. A. H. Hausrath acting in the capacity of project leader. Mr. Dittoe performed most of the first-phase work of this particular volume. The second phase of the overall project was performed mainly by G. W. Smith and E. E. Spier with Mr. Smith assigned as project leader. Valuable contributions were also made by Dr. S. N. Dharmarajan and Dr. P. E. Wilson who collaborated in the verification of the Langley buckling equation. The extension of this solution to include external running shear load was done solely by Dr. Dharmarajan.

During the overall effort, programming for the digital computer was accomplished mainly by Mrs. L. S. Fossum, Mrs. E. A. Muscha, and Mrs. N. L. Fraser, all of the Technical Programming Group. Mr. J. R. Anderson of the Guidance and Trajectory Programming Group also contributed.

Appreciation is expressed to H. L. Billmayer and H. R. Coldwater of the Structures Division, Propulsion and Vehicle Engineering Laboratory, Marshall Space Flight Center, for their support of the entire project. In the role of NASA Technical Representative, Mr. Billmayer provided helpful assistance in the definition and achievement of the study goals.

All six volumes of this report were typed by Mrs. F. C. Jaeger of the Convair Structural Analysis Group.

GDC-DDG-67-006

THE STABILITY OF ECCENTRICALLY STIFFENED CIRCULAR CYLINDERS

VOLUME VI

INTERACTION BEHAVIOR

By

G. W. Smith, E. E. Spier,
S. N. Dharmarajan, and L. S. Fossum
General Dynamics Convair Division
San Diego, California

ABSTRACT

This is the last of six volumes, each bearing the same report number, but dealing with separate problem areas concerning the stability of eccentrically stiffened circular cylinders. The complete set of documents was prepared under NASA Contract NAS8-11181. This particular volume includes a digital computer program which determines critical combinations of axial load (tension or compression) and radial pressure (bursting or crushing). The theoretical basis for this program is a solution developed by the NASA Langley Research Center. No consideration is given to the influences of pre-buckling distortions from the true cylindrical shape. Under the sponsorship of the NASA Marshall Space Flight Center, the General Dynamics Convair Division has extended the foregoing theoretical solution to incorporate the influences of external running shear acting either alone or in combination with axial load and/or radial pressure. The extended solution is also presented here. In addition, some discussion is given of the case where eccentrically stiffened cylinders are subjected to overall bending acting either alone or in combination with axial load.

TABLE OF CONTENTS

Preceding page blank

LIST OF ILLUSTRATIONS

Preceding page blank

DEFINITION OF SYMBOLS

Symbol	Definition
A_m	Amplitude of buckling displacement component [see equations (2-12)].
A_r	Cross-sectional area of single ring (no cylindrical skin included).
A_s	Cross-sectional area of single stringer (no cylindrical skin included).
$A_{11}, A_{12}, A_{13}, A_{22}, A_{23}, A_{33}$	Parameters defined by equations (2-11).
a	Overall length of cylinder.
a_n	Amplitude of buckling displacement component [see equations (2-18)].
B_m	Amplitude of buckling displacement component [see equations (2-12)].
b_n	Amplitude of buckling displacement component [see equations (2-18)].
C_m	Amplitude of buckling displacement component [see equations (2-12)].
c_n	Amplitude of buckling displacement component [see equations (2-18)].
D_m	Amplitude of buckling displacement component [see equations (2-12)].

Preceding page blank

DEFINITION OF SYMBOLS (Continued)

Symbol	Definition
D_x, D_y	Bending stiffnesses of basic cylindrical skin in longitudinal and circumferential directions, respectively. (For isotropic skins, $D_x = D_y = Et^3/12$).
D_{xy}	Twisting stiffness of basic cylindrical skin (For isotropic skins, $D_{xy} = Gt^3/6$).
d	Stringer spacing.
E	Young's modulus.
E_m	Amplitude of buckling displacement component [see equations (2-12)].
E_r	Young's modulus for ring.
E_s	Young's modulus for stringer.
E_x, E_y	Extensional stiffnesses of basic cylindrical skin in longitudinal and circumferential directions, respectively. (For isotropic skins, $E_x = E_y = Et$).
F_m	Amplitude of buckling displacement component [see equations (2-12)].
G	Modulus of elasticity in shear.
G(m)	Parameter defined by equation (2-15).
G_r	Ring modulus of elasticity in shear.
G_s	Stringer modulus of elasticity in shear.
G_{xy}	In-surface shear stiffness of basic cylindrical skin (For isotropic skins, $G_{xy} = Gt$).

DEFINITION OF SYMBOLS
(Continued)

Symbol	Definition
I_{o_r}	Moment of inertia of single ring (no cylindrical skin included) taken about middle surface of basic cylindrical skin.
I_{o_s}	Moment of inertia of single stringer (no cylindrical skin included) taken about middle surface of basic cylindrical skin.
$\bar{I}_r$	Centroidal moment of inertia of single ring (no cylindrical skin included)
$\bar{I}_s$	Centroidal moment of inertia of single stringer (no cylindrical skin included).
J_r	Torsional constant of single ring (no cylindrical skin included).
J_s	Torsional constant of single stringer (no cylindrical skin included).
ℓ	Ring spacing.
M_x, M_y, M_{xy}	Bending and twisting stress resultants of basic cylindrical skin.
m	Number of axial half-waves in buckle pattern; summation index.
N_x, N_y, N_{xy}	Normal and in-surface shear stress resultants of basic cylindrical skin.

DEFINITION OF SYMBOLS (Continued)

Symbol	Definition
$\bar{N}_x$	Uniformly distributed applied longitudinal running load acting at the centroid of skin-stringer combination (positive for compression; negative for tension).
$\bar{N}_{x_b}$	Peak value of non-uniformly distributed component of applied longitudinal running load acting at the centroid of skin-stringer combination [see equation (2-17)]; (positive for compression; negative for tension).
$\bar{N}_{x_c}$	Value of uniformly distributed component of applied longitudinal running load acting at the centroid of skin-stringer combination [see equation (2-17)]; (positive for compression; negative for tension).
$\left(\bar{N}_x\right)_{c+b}$	See equation (2-17).
$\bar{N}_{x_o}$	Critical value of uniformly distributed longitudinal running load $\bar{N}_x$ when acting alone.
$\bar{N}_{xy}$.	Uniform running shear load due to applied overall external torque acting about axis of revolution.
$\bar{N}_y$	Uniformly distributed applied circumferential running load acting at the centroid of the skin-ring combination (positive for compression; negative for tension).

DEFINITION OF SYMBOLS
(Continued)

Symbol	Definition
$\bar{N}_{y_o}$	Critical value of uniformly distributed circumferential running load $\bar{N}_y$ when acting alone.
n	Number of circumferential full-waves in buckle pattern; summation index.
R	Radius to middle surface of basic cylindrical skin.
R_x	Ratio of applied axial loading $(\bar{N}_x)$ to the critical value of axial loading when acting alone $(\bar{N}_{x_o})$
R_y	Ratio of applied circumferential loading $(\bar{N}_y)$ to the critical value of circumferential loading when acting alone $(\bar{N}_{y_o})$.
R_1 or R_2	Ratio of an applied load (or stress) to the critical value for that type of load (or stress) when acting alone.
t	Thickness of basic cylindrical skin.
u,v,w	Displacements in the x, y, and z directions, respectively, of a point in middle surface of basic cylindrical skin.
$\bar{u}$, $\bar{v}$, $\bar{w}$	Amplitudes of buckling displacements [see equations (2-9)].
x,y,z	Longitudinal, circumferential, and radial directions, respectively.
$\bar{z}_r$	Distance from centroid of ring (no basic cylindrical skin included) to middle surface of basic cylindrical skin (positive for external rings; negative for internal rings).

DEFINITION OF SYMBOLS
(Continued)

Symbol	Definition
$\bar{z}_s$	Distance from centroid of stringer (no basic cylindrical skin included) to middle surface of basic cylindrical skin (positive for external stringers; negative for internal stringers).
Γ_{Axial}	Knock-down factor for circular cylinder subjected to pure axial load (see Volume V).
Γ_{Bend}	Knock-down factor for circular cylinder subjected to pure bending (see Volume V).
δ_{jn}	Quantity defined by equations (2-21).
δ_{pm}	Quantity defined by equations (2-16).
$\epsilon_x, \epsilon_y, \gamma_{xy}$	Strains at middle surface of basic cylindrical skin.
ϵ_{x_s}	Longitudinal strain of stringer.
ϵ_{y_r}	Circumferential strain of ring.
μ	Poisson's ratio (For isotropic material).
μ_x, μ_y	Poisson's ratios for bending of orthotropic skin in longitudinal and circumferential directions, respectively (For isotropic skins, $\mu_x = \mu_y = \mu_x' = \mu_y' = \mu$).
μ_x', μ_y'	Poisson's ratios for extension of orthotropic skin in longitudinal and circumferential directions, respectively. (For isotropic skins, $\mu_x = \mu_y = \mu_x' = \mu_y' = \mu$).
π	Total change (due to buckling displacements) in potential energy of loaded stiffened cylinder (Also used as conventional notation for the constant 3.14 ---).
π_c	Change (due to buckling displacements) in strain energy of basic cylindrical skin.

DEFINITION OF SYMBOLS (Continued)

Symbol	Definition
π_L	Change (due to buckling displacements) in potential energy of external loading.
π_r	Change (due to buckling displacements) in strain energy of rings.
π_s	Change (due to buckling displacements) in strain energy of stringers.
σ_{cr}	Critical buckling stress

NOTE: A subscript preceded by a comma denotes partial differentiation with respect to the subscript variable. For example,

$$w_{,xy} = \frac{\partial^2 w}{\partial x \partial y} .$$

SECTION 1

INTRODUCTION

For isotropic cylinders that are subjected to combined external loads, it is customary to represent the critical loading combinations by means of so-called interaction curves. Figure 1 shows the graphical format usually employed for this purpose.

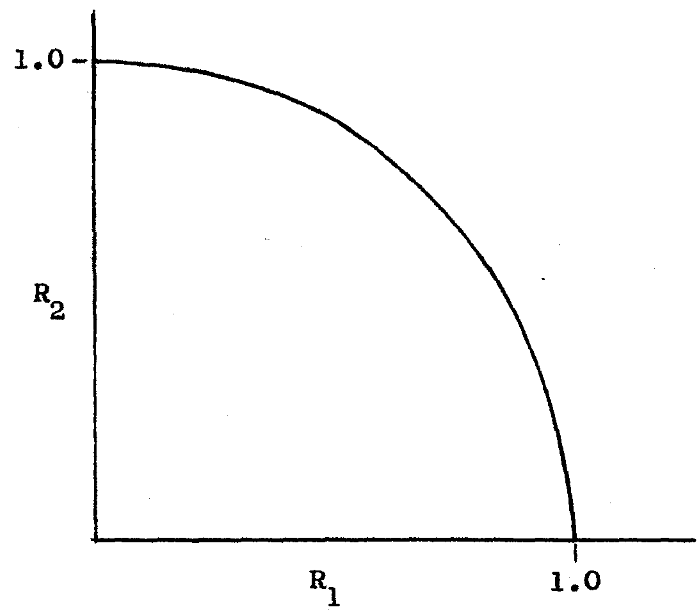

Figure 1 - Sample Interaction Curve for Isotropic Cylinders

The quantity R_1 is the ratio of an applied load or stress to the critical value for that type of loading when acting alone. The quantity R_2 is similarly defined for a second type of loading. Curves of this type give a very clear picture as to the structural integrity of particular configurations. All computed points which fall within the area bounded by the interaction curve and the coordinate axes correspond to stable structures. All points lying outside this region indicate that buckling will occur. Furthermore, a measure of the margin of safety is given by the ratio of distances from the calculated point to the curve and the origin. In view of the history of satisfactory experience with this type of curve in the design

and analysis of isotropic cylinders, it is quite natural to consider the application of this concept to eccentrically stiffened cylinders that are subjected to combined loads. However, whereas the behavior of isotropic cylinders can be adequately covered by a single curve for each two-load combination, the findings reported in this volume show that a multiplicity of curves is required for each two-load combination applied to eccentrically stiffened circular cylinders. This complexity arises out of the greater number of independent variables required to describe the physical features of the latter configurations. To keep the number of such curves within reasonable bounds, one must resort to simplifications which result, of course, in a loss of rigor. However, sufficient accuracy can be retained to make such curves useful for initial sizing, rough checking, and the study of trends. For the purposes of a final design, more refined values would be required. In general, these can only be obtained as single-point solutions from digital computer programs.

SECTION 2

EQUATIONS

2.1 COMBINED AXIAL LOAD AND RADIAL PRESSURE

The theoretical solution by Block, Card, and Mikulas [1] provides a suitable means for the stability analysis of eccentrically stiffened circular cylinders that are subjected to combined axial load (tension or compression) and radial pressure (bursting or crushing). This solution has been verified through the rederivation of reference 2. In general, the development by Block, et al. [1] was accomplished by the application of variational techniques to establish bifurcation points (see Volume I [3]) along an initially linear equilibrium path. This was achieved by first formulating expressions for the changes in strain energy due to the buckling displacements. For the basic cylindrical skin this increment was expressed as follows:

$$\pi_c = \frac{1}{2}\int_0^{2\pi R}\int_0^{a} (N_x\varepsilon_x + N_{xy}\gamma_{xy} + N_y\varepsilon_y - M_x w_{,xx} + 2M_{xy}w_{,xy} - M_y w_{,yy})\, dx\, dy \tag{2.1}$$

where

N_x, N_{xy}, N_y, M_x, M_{xy}, M_y = Stress resultants of basic cylindrical skin.

ε_x, ε_y, γ_{xy} = Strains at middle surface of basic cylindrical skin.

π_c = Change (due to buckling displacements) in strain energy of basic cylindrical skin.

x = Longitudinal direction.

y = Circumferential direction.

R = Cylinder radius.

a = Overall length of cylinder.

Numbers in brackets [ ] in the text denote references listed in SECTION 6.

The manner in which Block, et al [1] formulate the stress resultants facilitates analysis where the basic cylindrical skins themselves have orthotropic properties. Proceding then to the longitudinal stiffeners, their change in strain energy was expressed as follows:

$$\pi_s = \frac{1}{2}\int_0^{2\pi R}\int_0^{a}\left(\int_{A_s} \frac{E_s \varepsilon_{x_s}^2}{d}\, dA_s + \frac{G_s J_s}{d}\, w_{,xy}^{\;2}\right) dxdy \tag{2-2}$$

where

π_s = Change (due to buckling displacements) in strain energy of longitudinal stiffeners.

A_s = Cross-sectional area of longitudinal stiffener (no cylindrical skin included).

ε_{x_s} = Longitudinal strain of longitudinal stiffener.

d = Stringer spacing.

G_s = Shear modulus of longitudinal stiffener.

J_s = Torsional constant of longitudinal stiffener.

w = Radial displacement.

The change in strain energy of the circumferential stiffeners was found from

$$\pi_r = \frac{1}{2}\int_0^{2\pi R}\int_0^{a}\left(\int_{A_r} \frac{E_r \varepsilon_{y_r}^2}{\ell}\, dA_r + \frac{G_r J_r}{\ell}\, w_{,xy}^{\;2}\right) dxdy \tag{2-3}$$

where

ℓ = Ring spacing

r = Subscript denoting ring (circumferential stiffener not including any cylindrical skin).

The change in the potential energy of the external loading was taken as

$$\pi_L = -\frac{1}{2}\int_0^{2\pi R}\int_0^{a}\left(\bar{N}_x w,_x{}^2 + 2\bar{N}_{xy} w,_x w,_y + \bar{N}_y w,_y{}^2\right) dx\, dy \qquad (2\text{-}4)$$

where

π_L = Change (due to buckling displacements) in potential energy of external loading.

$\bar{N}_x$ = Applied running axial load.

$\bar{N}_y$ = Applied running hoop load.

$\bar{N}_{xy}$ = Applied running in-surface shear load.

Although this expression includes the applied running shear load $\bar{N}_{xy}$, Block, et al. [1] later set this term equal to zero so that their final equation applies only to the case of applied axial load and/or applied radial pressure.

By making use of equations (2-1) through (2-4), the total potential energy of the system was expressed as follows:

$$\pi = \pi_c + \pi_s + \pi_r + \pi_L \qquad (2\text{-}5)$$

The next step was to employ the principle of stationary potential energy (see Volume I [3]) to arrive at the following set of equilibrium equations in terms of the buckling displacements u, v, and w:

$$\frac{E_x}{1-\mu_x'\mu_y'} u,_{xx} + \frac{E_s A_s}{d}\left(u,_{xx} - \bar{z}_s w,_{xxx}\right)$$

$$+ \frac{\mu_y' E_x}{1-\mu_x'\mu_y'}\left(v,_{xy} + \frac{w,_x}{R}\right) + G_{xy}\left(u,_{yy} + v,_{xy}\right) = 0 \qquad (2\text{-}6)$$

$$\frac{E_y}{1-\mu_x'\mu_y'}\left(v_{,yy}+\frac{w_{,y}}{R}\right)+\frac{E_rA_r}{\ell}\left(v_{,yy}+\frac{w_{,y}}{R}-\bar{z}_r w_{,yyy}\right)$$

$$+\frac{\mu_x'E_y}{1-\mu_x'\mu_y'}\,u_{,xy}+G_{xy}\left(u_{,xy}+v_{,xx}\right)=0 \qquad (2\text{-}7)$$

$$\left(\frac{D_x}{1-\mu_x\mu_y}+\frac{E_sI_{o_s}}{d}\right)w_{,xxxx}+\left(\frac{\mu_yD_x}{1-\mu_x\mu_y}+2D_{xy}+\frac{\mu_xD_y}{1-\mu_x\mu_y}+\frac{G_sJ_s}{d}+\frac{G_rJ_r}{\ell}\right)w_{,xxyy}$$

$$+\left(\frac{D_y}{1-\mu_x\mu_y}+\frac{E_rI_{o_r}}{\ell}\right)w_{,yyyy}+\frac{E_y}{R(1-\mu_x'\mu_y')}\left(\mu_x'u_{,x}+v_{,y}+\frac{w}{R}\right)$$

$$-\frac{E_sA_s}{d}\bar{z}_s u_{,xxx}-\frac{E_rA_r}{\ell}\bar{z}_r\left(\frac{2w_{,yy}}{R}+v_{,yyy}\right)+\frac{E_rA_r}{R\ell}\left(v_{,y}+\frac{w}{R}\right)$$

$$+\bar{N}_x w_{,xx}+2\bar{N}_{xy}w_{,xy}+\bar{N}_y w_{,yy}=0 \qquad (2\text{-}8)$$

Block, et al. [1] then obtained a solution to these equations by assuming boundary conditions of classical simple support and the following set of buckling displacement functions:

$$\begin{aligned} u &= \bar{u}\cos\frac{m\pi x}{a}\cos\frac{ny}{R} \\ v &= \bar{v}\sin\frac{m\pi x}{a}\sin\frac{ny}{R} \\ w &= \bar{w}\sin\frac{m\pi x}{a}\cos\frac{ny}{R} \end{aligned} \qquad (2\text{-}9)$$

where

m = Number of longitudinal half-waves in buckle pattern.

n = Number of circumferential full-waves in the buckle pattern.

By substituting equations (2-9) into the equilibrium equations, it can be observed that the existence of non-trivial buckling displacements requires that a certain determinant vanish. This condition reduces to the stability equation

$$\left(\frac{m\pi}{a}\right)^2 \bar{N}_x + \left(\frac{n}{R}\right)^2 \bar{N}_y = A_{33} + \left(\frac{A_{12}A_{23}-A_{13}A_{22}}{A_{11}A_{22}-A_{12}^2}\right) A_{13} + \left(\frac{A_{12}A_{13}-A_{11}A_{23}}{A_{11}A_{22}-A_{12}^2}\right) A_{23} \tag{2-10}$$

where the A_{ij}'s are functions of the material properties, the geometry of the cylinder, and the shape of the buckle pattern. In particular, these quantities can be expressed as follows:

$$\begin{aligned}
A_{11} &= \left(\frac{E_x}{1-\mu_x'\mu_y'} + \frac{E_s A_s}{d}\right)\left(\frac{m\pi}{a}\right)^2 + G_{xy}\left(\frac{n}{R}\right)^2 \\
A_{12} &= \left(\frac{\mu_y' E_x}{1-\mu_x'\mu_y'} + G_{xy}\right)\left(\frac{m\pi}{a}\right)\left(\frac{n}{R}\right) \\
A_{13} &= \frac{1}{R}\left(\frac{\mu_y' E_x}{1-\mu_x'\mu_y'}\right)\left(\frac{m\pi}{a}\right) + \frac{E_s A_s}{d}\bar{z}_s\left(\frac{m\pi}{a}\right)^3
\end{aligned} \tag{2-11}$$

$$A_{22} = G_{xy}\left(\frac{m\pi}{a}\right)^2 + \left(\left(\frac{E_y}{1-\mu_x'\mu_y'} + \frac{E_rA_r}{\ell}\right)\left(\frac{n}{R}\right)\right)^2$$

(2-11) Cont'd

$$A_{23} = \frac{1}{R}\left(\frac{E_y}{1-\mu_x'\mu_y'} + \frac{E_rA_r}{\ell}\right)\left(\frac{n}{R}\right) + \frac{E_rA_r}{\ell}\bar{z}_r\left(\frac{n}{R}\right)^3$$

$$A_{33} = \left(\frac{D_x}{1-\mu_x\mu_y} + \frac{E_sI_{o_s}}{d}\right)\left(\frac{m\pi}{a}\right)^4 + \left(\frac{2\mu_yD_x}{1-\mu_x\mu_y} + 2D_{xy} + \frac{G_sJ_s}{d} + \frac{G_rJ_r}{\ell}\right)\left(\frac{m\pi}{a}\right)^2\left(\frac{n}{R}\right)^2$$
$$+\left(\frac{D_y}{1-\mu_x\mu_y} + \frac{E_rI_{o_r}}{\ell}\right)\left(\frac{n}{R}\right)^4 + \frac{1}{R^2}\left(\frac{E_y}{1-\mu_x'\mu_y'} + \frac{E_rA_r}{\ell}\right) + 2\,\frac{E_rA_r}{\ell}\bar{z}_r\frac{n^2}{R^3}$$

Note that the foregoing A_{ij}'s are not the elastic constants defined in Volume I [3] and used elsewhere throughout this multiple-volume report.

Equation (2-10) is the fundamental buckling criterion that emerges from the derivation of Block, et al. [1]. It should be observed that this equation does nothing more than establish $\bar{N}_x$ and $\bar{N}_y$ values which are capable of maintaining the cylinder in deformed configurations which correspond to particular numbers of longitudinal half-waves m and circumferential full waves n . Calling upon the bifurcation concept discussed in Volume I [3], it follows that the critical buckling loads can be established by exploring the possible deformed equilibrium configurations for a minimum load condition. The digital computer program of SECTION 5 makes use of equation (2-10) in precisely this manner. Through the input, the analyst prescribes the ranges of m and n to be explored. The machine then computes the $\bar{N}_x$ or $\bar{N}_y$ values corresponding to each included m-n combination and prints out the lowermost load encountered. Further refinement to this program could easily be

accomplished to eliminate the prior judgements required of the user in selecting appropriate ranges of m and n to be screened.

Although the foregoing solution can be considered suitable for the purposes of final design, it is not intended that the reader interpret this to mean that equation (2-10) is perfectly rigorous. At best, it represents a state-of-the-art operational capability in a rapidly changing technology. For one thing, it should be noted that this solution is based on small-deflection theory. Hence, the theoretical results obtained from equation (2-10) must be reduced by appropriate knock-down factors (see Volume V [4])to account for the detrimental effects of initial imperfections. Furthermore, the subject solution is based upon the complete neglect of non-cylindrical pre-buckling distortions which can be extremely important where pressure differentials exist across the shell wall. End and ring restraint to Poisson's-ratio hoop growth further contribute to this type of pre-buckling deformation. It should also be observed that the solution of Block, et al.[1] is primarily based upon monocoque shell theory and its application to discretely stiffened cylinders is achieved by the conventional smearing-out technique. For this purpose, the stiffnesses of the discrete component members are averaged over the entire shell surface to obtain an equivalent monocoque analysis model. In view of this, it might sometimes be wise to consider the introduction of modified component section properties to arrive at true equivalence. Influences from such sources as shear lag, stiffener attachment techniques, etc. might be reflected into the analysis by such modifications. Finally, it should be noted that the solution of Block et al. [1] is based upon Donnell-type simplifications which render the results invalid for non-axisymmetric buckle patterns having a small number of circumferential waves. The rule-of-thumb guideline is offered here that this solution be considered inapplicable for cases where $0 < n < 2$.

2.2 COMBINED AXIAL LOAD, RADIAL PRESSURE, AND RUNNING SHEAR

To analyze this case of combined loading, the theoretical solution of reference 2 may be used. This solution constitutes an extension to the theory of Block, et al. [1] which is discussed in SECTION 2.1 above. To accomplish this extension, use was made of the same equilibrium equations as were employed by Block, et al. These expressions are given above as

equations (2-6), (2-7), and (2-8). Then, unlike the derivation of reference 1, the $\bar{N}_{xy}$ term was retained throughout all of the subsequent mathematical operations. The presence of this additional term made it necessary to introduce displacement functions which differ from those expressed as equations (2-9). In particular, the following formulations were selected:

$$u = \sin\frac{ny}{R}\sum_{m=1,3,--}^{\infty} A_m \cos\frac{m\pi x}{a} + \cos\frac{ny}{R}\sum_{m=2,4,---}^{\infty} E_m \cos\frac{m\pi x}{a}$$

$$v = \cos\frac{ny}{R}\sum_{m=1,3,---}^{\infty} B_m \sin\frac{m\pi x}{a} + \sin\frac{ny}{R}\sum_{m=2,4,---}^{\infty} F_m \sin\frac{m\pi x}{a} \qquad (2\text{-}12)$$

$$w = \sin\frac{ny}{R}\sum_{m=1,3,--}^{\infty} C_m \sin\frac{m\pi x}{a} + \cos\frac{ny}{R}\sum_{m=2,4,--}^{\infty} D_m \sin\frac{m\pi x}{a}$$

These equations satisfy the boundary conditions of classical simple support. By substituting equations (2-12) into the equilibrium equations and by applying the Galerkin method [5], one can obtain the following set of homogeneous equations [2]:

$$\frac{a}{2}\sum_{m=1,3,--}^{\infty} G(m)\, C_m\, \delta_{pm} - 4\bar{N}_{xy}\frac{n}{R}\sum_{m=2,4,--}^{\infty} \frac{mp}{p^2-m^2} D_m = 0 \quad (p = 1,3,5,---) \qquad (2\text{-}13$$

$$\frac{a}{2}\sum_{m=2,4,--}^{\infty} G(m)\, D_m\delta_{pm} + 4\bar{N}_{xy}\frac{n}{R}\sum_{m=1,3,--}^{\infty} \frac{mp}{p^2-m^2} C_m = 0 \quad (p = 2,4,6,---) \qquad (2\text{-}14$$

where

$$G(m) = A_{33} - \frac{A_{23}(A_{11}A_{23} - A_{13}A_{12}) + A_{13}\ (A_{22}A_{13} - A_{23}A_{12})}{A_{11}A_{22} - A_{12}^{\ 2}} - \bar{N}_x\left(\frac{m\pi}{a}\right)^2 - \bar{N}_y\left(\frac{n}{R}\right)^2 \qquad (2\text{-}15)$$

and

$$\begin{aligned} \delta_{pm} &= 1 \quad \text{if } p=m \\ \delta_{pm} &= 0 \quad \text{if } p\neq m \end{aligned} \qquad (2\text{-}16)$$

The A_{ij}'s of equation (2-15) are the same quantities as were previously defined by equations (2-11).

Equations (2-13) through (2-16) furnish a theoretical basis for computing the buckling loads of eccentrically stiffened circular cylinders which are subjected to combined axial load and/or radial pressure and/or running shear. It should be noted that these relatively compact equations actually represent an infinite system of homogeneous algebraic equations and, from a practical standpoint, one must rely upon a digital computer to obtain numerical results. A typical application might involve the computation of a critical $\bar{N}_{xy}$ in the presence of given $\bar{N}_x$ and $\bar{N}_y$ loadings. The desired critical value would be the lowest eigenvalue $\bar{N}_{xy}$ for the determinant of the coefficients for C_m and D_m. In general, the larger the selected determinant, the better is the accuracy but the greater is the computational effort (computer machine-time).

No digital computer program is furnished here to implement the foregoing analysis method. It is therefore recommended that such a program be developed in the near future. Note however that, since the above results constitute an extension to the basic development of Block et al. [1], all of the limitations cited in SECTION 2.1 apply here as well.

2.3 COMBINED AXIAL LOAD AND OVERALL BENDING

In order to properly understand the state-of-the-art relative to this combined loading condition, it is helpful to first consider the current status for stiffened cylinders subjected only to pure bending. To begin with,

it is pointed out that some disagreement exists among the recently published documents concerning this problem. On the one hand, the theoretical results of reference 6 indicate that the critical stresses for orthotropic cylinders under pure bending are equal to the critical values for pure axial compression. This is contrary to the findings of Hedgepeth and Hall [7] for a particular corrugated cylinder having internal rings. For pure bending, these theoretical results show a buckling stress which is approximately 1.23 times the buckling stress under uniform axial loading. Still another theoretical development was recently published by Block [8] which similarly shows differences between the critical stresses for the two subject loading conditions. The theory developed by Block [8] is an extension to the basic approach of reference 1. The same governing differential equations of equilibrium were employed. These expressions are given above as equations (2-6), (2-7), and (2-8). The values $\overline{N}_{xy}$ and $\overline{N}_y$ were each set equal to zero and $\overline{N}_x$ was expressed in a form equivalent to

$$\left(\overline{N}_x\right)_{c+b} = \overline{N}_{x_c} + \overline{N}_{x_b} \cos \frac{y}{R} \qquad (2\text{-}17)$$

This permits consideration of overall bending acting either alone or in combination with uniform axial loading $\overline{N}_{x_c}$. The quantity $\overline{N}_{x_b}$ is the peak running compressive loading due to the overall bending moment. In the solution of reference 8, the following expressions were used to describe the buckling displacements u, v, and w:

$$u = \cos \frac{m\pi x}{a} \sum_{n=0}^{\infty} c_n \cos \frac{ny}{R}$$

$$v = \sin \frac{m\pi x}{a} \sum_{n=0}^{\infty} b_n \sin \frac{ny}{R} \qquad (2\text{-}18)$$

$$w = \sin \frac{m\pi x}{a} \sum_{n=0}^{\infty} a_n \cos \frac{ny}{R}$$

By substituting these functions into the equilibrium equations and applying the Galerkin method [5], Block obtained the following final expressions:

$$a_n\left(F_n - \bar{N}_{x_c}\right) - \frac{\bar{N}_{x_b}}{2}\left[\left(1 + \delta_{1n} - \delta_{0n}\right)a_{n-1} + a_{n+1}\right] = 0 \qquad (2\text{-}19)$$

where

$$F_n = \left(\frac{a}{m\pi}\right)^2\left[A_{33} + A_{23}\left(\frac{A_{12}A_{13} - A_{11}A_{23}}{A_{11}A_{22} - A_{12}^{\,2}}\right) + A_{13}\left(\frac{A_{12}A_{23} - A_{13}A_{22}}{A_{11}A_{22} - A_{12}^{\,2}}\right)\right] \qquad (2\text{-}20)$$

and

$$\begin{aligned} &n = 0,1,2,3,\ldots \\ &\delta_{jn} = 1 \quad \text{if} \quad (j = n) \\ &\delta_{jn} = 0 \quad \text{if} \quad (j \neq n) \end{aligned} \qquad (2\text{-}21)$$

The A_{ij}'s of equation (2-20) are the same quantities as were previously defined by equations (2-11).

Just as in the combined loading analysis cited in SECTION 2.2 above, the relatively compact equations (2-19) through (2-21) actually represent an infinite system of homogeneous algebraic equations. Here again, from a practical standpoint, one must rely upon a digital computer to establish numerical values for the critical loadings. As before, the size of the selected system of equations will determine the accuracy obtained and the computational effort (computer machine-time) required.

The basic nature of the numerical techniques involved in the application of equations (2-13) through (2-16) is the same as that associated with equations (2-19) through (2-21). To understand the fundamental approach, the latter set of equations will be further discussed. In this connection, it should be recalled that a set of homogeneous algebraic equations can have a nontrivial solution if, and only if, the determinant of the coefficients equals zero. Hence, in the case of equations (2-19) through (2-21), one

might first assemble the determinant of the coefficients for the a_i's. This determinant could then be expanded and set equal to zero to obtain a polynomial equation in which, for given m and n values, either $\overline{N}_{x_c}$ or $\overline{N}_{x_b}$ is the only unknown. For any single m-n combination, the lowermost root of this equation could then be computed. Such computations might be repeated for all possible m-n combinations. The critical loading would be the lowermost value encountered in this screening type of operation. Although this procedure is relatively simple in concept, it is often quite difficult to actually determine the lowermost roots of the polynomial equations, particularly when the size of the selected determinant is large. Therefore, mathematicians have devised a number of numerical schemes to extract these roots (eigenvalues) from the determinantal equation. Most computer laboratories have on-the-shelf sub-routines to perform such operations and they will not be discussed any further here.

Following his derivation of equations (2-19) through (2-21), Block [8] then computed some sample results for three contemporary types of eccentrically stiffened circular cylinders: ring-stiffened corrugated cylinders, ring-and-stringer-stiffened cylinders, and longitudinally (stringer) stiffened cylinders. Like the results given in reference 7, Block [8] obtained different critical stresses for the separate cases of pure axial load and pure bending moment. The ratios of

$$\frac{\text{Pure Bending } \sigma_{cr}}{\text{Pure Compression } \sigma_{cr}}$$

ranged from 1.013 up to 1.397.

To place the contents of this particular section in a proper perspective, it might be noted here that the historical development of isotropic cylinder theory likewise involved some controversy as to the relative theoretical strengths for the separate cases of pure axial load and pure bending moment. An analysis presented in references 9 and 10 indicated that,

for an assumed buckle waveform, the critical stress for isotropic cylinders under pure bending was 1.3 times the critical stress for pure compression. This calculation was cited by Timoshenko [11] without a qualifying statement as to the assumed buckle wavelength. Because test data seemed to substantiate the existence of such an increase, the 1.3 factor was used for decades as a generally applicable value. However, the small-deflection analysis of reference 12 recently revealed that the ratio of critical bending and compression stresses can vary widely with longitudinal wavelengths and that properly minimized results show that the correct ratio is essentially equal to unity. The apparent increase of bending strength over compressive strength indicated by isotropic test data can only be explained by a consideration of the sensitivity to initial imperfections. For axially compressed isotropic cylinders these defects result in a severe reduction of actual strengths below classical theoretical values. Since, under pure bending, only a small portion of the cylinder's circumference experiences the peak stresses which initiate buckling, there is a statistical influence from the probability for defects to exist within this restricted region of the overall shell wall. As a result, it is reasonable to expect that, under pure bending, actual reductions below classical theoretical values will not be as severe as those for pure axial compression.

In view of all the factors cited in this section concerning the interaction behavior of stiffened cylinders and isotropic cylinders, it appears that, to facilitate the practical design and analysis of stiffened configurations, one might choose between the following two alternatives for cases of overall bending acting either alone or in combination with axial load:

(a) Assume that the theoretical critical stresses are the same for the separate cases of pure bending and pure axial compression. The only differences between allowable levels for these two cases would then result from the application of knock-down factors (see Volume V [4]) which recognize

differences in the probabilities for initial imperfections to coincide with peak stress locations. The related interaction curve would simply be taken as the straight line which intercepts the horizontal and vertical coordinate axes at values of unity.

(b) Obtain theoretical critical loadings from digital computer solutions based on the formulation of Block [8]. As noted earlier, this solution gives different critical stresses for the separate cases of pure bending and pure axial compression. Here again, knock-down factors would be applied using the criteria of Volume V [4]. These factors would further accentuate the differences between pure bending and pure compression. To be structurally sound, a given configuration must be capable of supporting the loading combination

$$\left(\frac{\text{Design } \bar{N}_{x_c}}{\Gamma_{Axial}} ; \frac{\text{Design } \bar{N}_{x_b}}{\Gamma_{Bend}} \right)$$

where

Γ_{Axial} = Knock-down factor for circular cylinder subjected to pure axial load (see Volume V [4]).

Γ_{Bend} = Knock-down factor for circular cylinder subjected to pure bending (see Volume V [4]).

The recommendation of this volume is that alternative (b) be followed. However, no digital computer program is furnished here to implement this recommendation. Furthermore, note that, since the subject formulation of Block [8] constitutes an extension to the basic approach of reference 1, most of the limitations cited in SECTION 2.1 apply here as well. Only those limitations related solely to the presence of pressure differentials are inapplicable to the case under discussion.

SECTION 3

PARAMETRIC STUDIES

In order to observe some of the trends of interaction behavior for eccentrically stiffened circular cylinders, several studies were conducted for the case of combined axial load and radial pressure. Both of the following combinations were considered:

(a) Axial compression plus radial crushing pressure.

(b) Axial compression plus radial bursting pressure.

These investigations were performed by using the digital computer program of SECTION 5. As noted earlier, this program is based on the theoretical solution of Block, et al. [1]. It should be recalled that this solution completely neglects the effects of non-cylindrical pre-buckling deformations such as arise out of the presence of pressure differentials and discrete stiffeners. Localized restraint to Poisson's ratio hoop growth likewise contributes to these discontinuity-type deformations. These two influences are likely to be quite important for all stiffened configurations except those where the stiffeners are very closely spaced.

The configurations studied here may be described in terms of the various input values to the digital computer program of SECTION 5. In particular, these are as follows:

<u>Configuration 1:</u>

R = Cylinder Radius = 38.6 in.

a = Overall Length = 72 in.

d = Stringer Spacing = 2.48 in.

ℓ = Ring Spacing = 6.00 in.

E_x	=	$1.5\text{x}10^6$ lbs/in.	E_y	=	$2\text{x}10^6$ lbs/in.
D_x	=	250 lb-in.	D_y	=	300 lb-in.
G_{xy}	=	$2\text{x}10^5$ psi	D_{xy}	=	182.25 lb-in.
μ_x'	=	0.25	μ_y'	=	0.35
μ_x	=	0.30	μ_y	=	0.40
E_s	=	$30\text{x}10^6$ psi	E_r	=	$25\text{x}10^6$ psi.
G_s	=	$12\text{x}10^6$ psi.	G_r	=	$10\text{x}10^6$ psi.
A_s	=	0.020 sq. in.	A_r	=	0.040 sq. in.

$I_{o_s} = 0.005 \text{ in.}^4$ $\qquad$ $I_{o_r} = 0.010 \text{ in.}^4$

$J_s = 0.004 \text{ in.}^4$ $\qquad$ $J_r = 0.006 \text{ in.}^4$

$\bar{z}_s = 0$ $\qquad$ $\bar{z}_r = 0$

<u>Configuration 2:</u>

Same as Configuration 1 except that

ℓ = Ring Spacing = 0.5 in.

<u>Configuration 3:</u>

Same as Configuration 1 except that

ℓ = Ring Spacing = 72 in.

Note that the eccentricity values for the above configurations are all taken equal to zero which means that the stiffener centroids are located in the middle surface of the basic cylindrical skin. To provide some insight into the influences from non-zero eccentricities, the following configurations were also included in the study:

<u>Configuration 4:</u>

Same as Configuration 1 except that

$\bar{z}_s = 0.50$ in. and $\bar{z}_r = 0.75$ in.

<u>Configuration 5:</u>

Same as Configuration 3 except that

$\bar{z}_s = 0.50$ in. and $\bar{z}_r = 0.75$ in.

Various critical combinations of applied axial compression ($\bar{N}_x$) and applied radial compression ($\bar{N}_y$) were determined for each of the preceding configurations so that interaction curves could be plotted. The results are tabulated in Table I and are plotted in Figure 2 where the appropriate configuration numbers are shown in parentheses. The quantity R_x is the ratio of applied axial loading ($\bar{N}_x$) to the critical value of axial loading when acting alone $\left(\bar{N}_{x_o}\right)$ and the quantity R_y is the ratio of applied circumferential loading ($\bar{N}_y$) to the critical value of circumferential loading

when acting alone $\left(\bar{N}_{y_o}\right)$. Observe that the interaction relationships cannot be expressed by a single curve. Even in the absence of eccentricities (configurations 1, 2, and 3), variations in the basic geometry led to different curves. The introduction of non-zero eccentricities resulted in further complication in that still a greater number of curves then emerged.

To study the combination of axial compression acting along with radial bursting pressure, solutions were obtained for the same five configurations as cited above. These results are tabulated in Table II and are plotted in Figure 3 where, once again, the appropriate configuration designations are shown in parentheses. The circumferential tensile loading due to internal pressure is shown nondimensionally in terms of the circumferential critical compressive loading $\left(\bar{N}_{y_o}\right)$. Here too, it can be seen that variations in the basic geometry (including eccentricity values) lead to different interaction curves.

TABLE I

Calculated Data for Interaction Example Configurations - Axial Compression and External Radial Pressure

CONFIGURATION	$\bar{N}_y$	$\bar{N}_x$	m	n	$\frac{\bar{N}_y}{\bar{N}_{y_o}}$	$\frac{\bar{N}_x}{\bar{N}_{x_o}}$
1	0	7868	4	7	0	1
	309	7452	3	7	.25	.947
	567	5901	1	5	.459	.75
	619	5450	1	5	.50	.693
	791	3934	1	5	.639	.50
	928	2725	1	5	.75	.346
	1014	1967	1	5	.820	.25
	1237	0	1	5	1	0
2	0	15157	5	5	0	1
	1761	14536	5	5	.25	.959
	3521	13915	5	5	.50	.918
	4983	11368	1	3	.708	.75
	5282	9931	1	4	.75	.655
	5699	7579	1	4	.809	.50
	6371	3789	1	4	.905	.25
	7042	0	1	4	1	0
3	0	4089	1	6	0	1
	62	3282	1	7	.25	.803
	74	3066	1	7	.301	.75
	124	2215	1	7	.50	.542
	185	1148	1	7	.75	.281
	193	1022	1	7	.780	.25
	219	560	1	7	.888	.137
	247	0	1	8	1	0

TABLE I
(Continued)

Calculated Data for
Interaction Example Configurations -
Axial Compression and External
Radial Pressure

CONFIGU-RATION	$\bar{N}_y$	$\bar{N}_x$	m	n	$\frac{\bar{N}_y}{\bar{N}_{y_o}}$	$\frac{\bar{N}_x}{\bar{N}_{x_o}}$
4	0	8347	3	7	0	1
	266	7396	1	5	.25	.886
	395	6260	1	5	.371	.75
	533	5049	1	5	.50	.605
	632	4174	1	5	.593	.50
	799	2701	1	5	.75	.324
	868	2086	1	5	.816	.25
	1065	0	1	6	1	0
5	0	4301	1	6	0	1
	62	3405	1	7	.25	.792
	125	2326	1	7	.50	.541
	187	1247	1	7	.75	.290
	225	564	1	8	.90	.131
	250	0	1	8	1	0

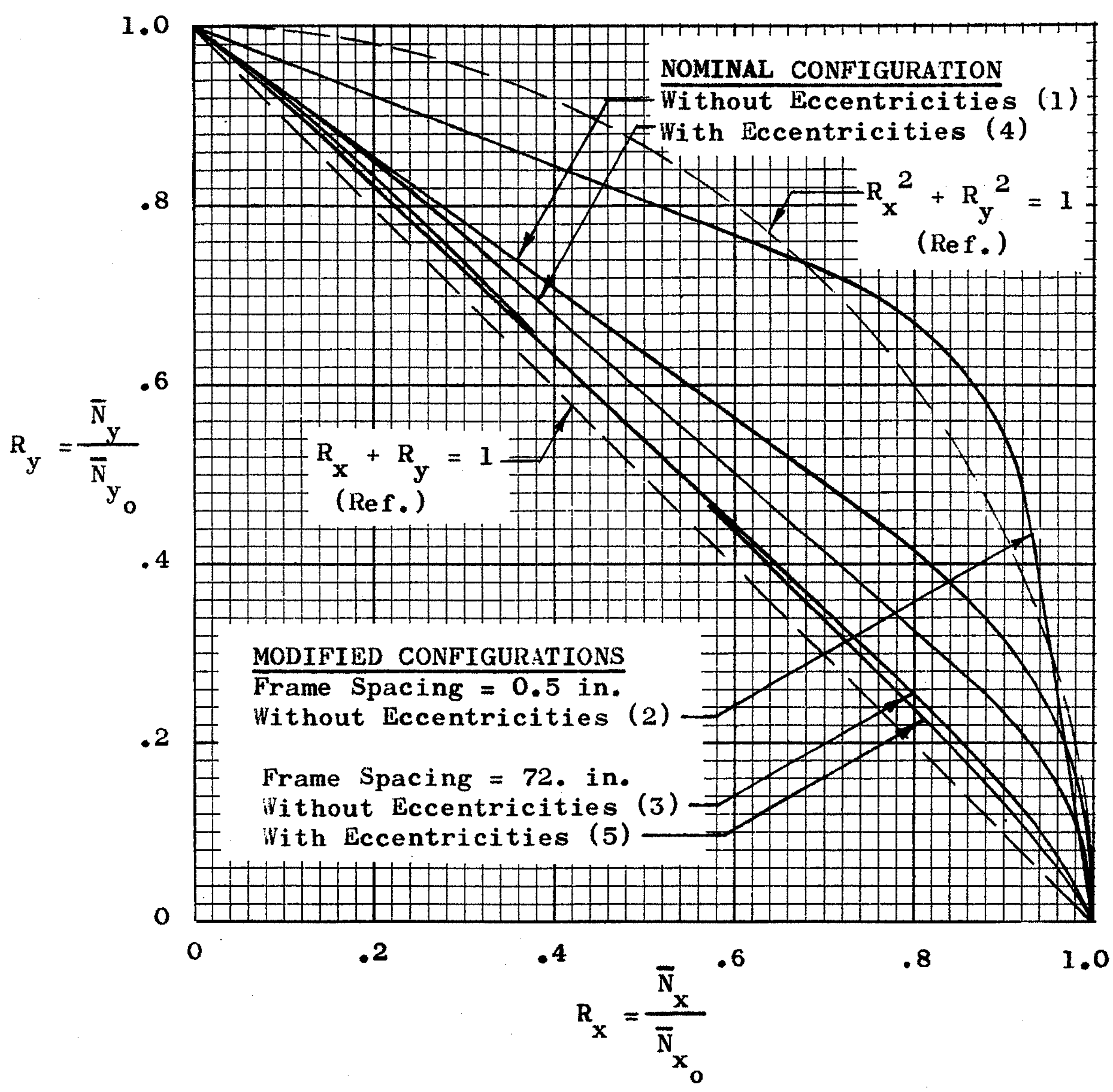

Figure 2 - Stability Interaction Results for Combined Axial Compression and External Radial Pressure

TABLE II

Calculated Data for Interaction Example Configurations - Axial Compression and Internal Radial Pressure

CONFIGURATION	$\bar{N}_y$	$\bar{N}_x$	m	n	$\frac{\bar{N}_y}{\bar{N}_{y_o}}$	$\frac{\bar{N}_x}{\bar{N}_{x_o}}$
1	1237	0	1	5	1	0
	0	7868	4	7	0	1
	-309	8202	4	7	-.25	1.042
	-618	8535	4	7	-.50	1.085
	-1237	9189	4	6	-1	1.168
	-2474	10,071	5	7	-2	1.280
	-4948	11,339	5	6	-4	1.441
	-12369	13,809	6	5	-10	1.755
2	7042	0	1	4	1	0
	0	15,157	5	5	0	1
	-1761	15,665	6	5	-.25	1.034
	-3521	16,096	6	5	-.50	1.062
	-7042	16,958	6	5	-1	1.119
	-14085	18,245	7	4	-2	1.204
	-28170	19,866	7	4	-4	1.311
	-70424	22,989	9	3	-10	1.517
3	247	0	1	8	1	0
	0	4089	1	6	0	1
	-62	4569	2	8	-.25	1.118
	-124	4917	2	8	-.50	1.203
	-247	5427	3	8	-1	1.327
	-494	6046	3	8	-2	1.479
	-988	7033	4	8	-4	1.720
	-2470	8868	4	7	-10	2.196

TABLE II
(Continued)

Calculated Data for Interaction Example Configurations - Axial Compression and Internal Radial Pressure

CONFIGU-RATION	$\bar{N}_y$	$\bar{N}_x$	m	n	$\frac{\bar{N}_y}{\bar{N}_{y_o}}$	$\frac{\bar{N}_x}{\bar{N}_{x_o}}$
4	1065	0	1	6	1	0
	0	8347	3	7	0	1
	- 266	8661	4	7	-.25	1.038
	- 533	8948	4	7	-.50	1.072
	-1065	9523	4	7	-1	1.141
	-2131	10,265	5	7	-2	1.230
	-4262	11,303	6	6	-4	1.354
	-10654	13,117	7	5	-10	1.571
5	250	0	1	8	1	0
	0	4301	1	6	0	1
	- 62	4938	2	8	-.25	1.148
	- 125	5290	2	8	-.50	1.230
	- 250	5848	3	8	-1	1.360
	- 500	6474	3	8	-2	1.505
	- 1000	7360	4	8	-4	1.711
	- 2499	8947	5	7	-10	2.080

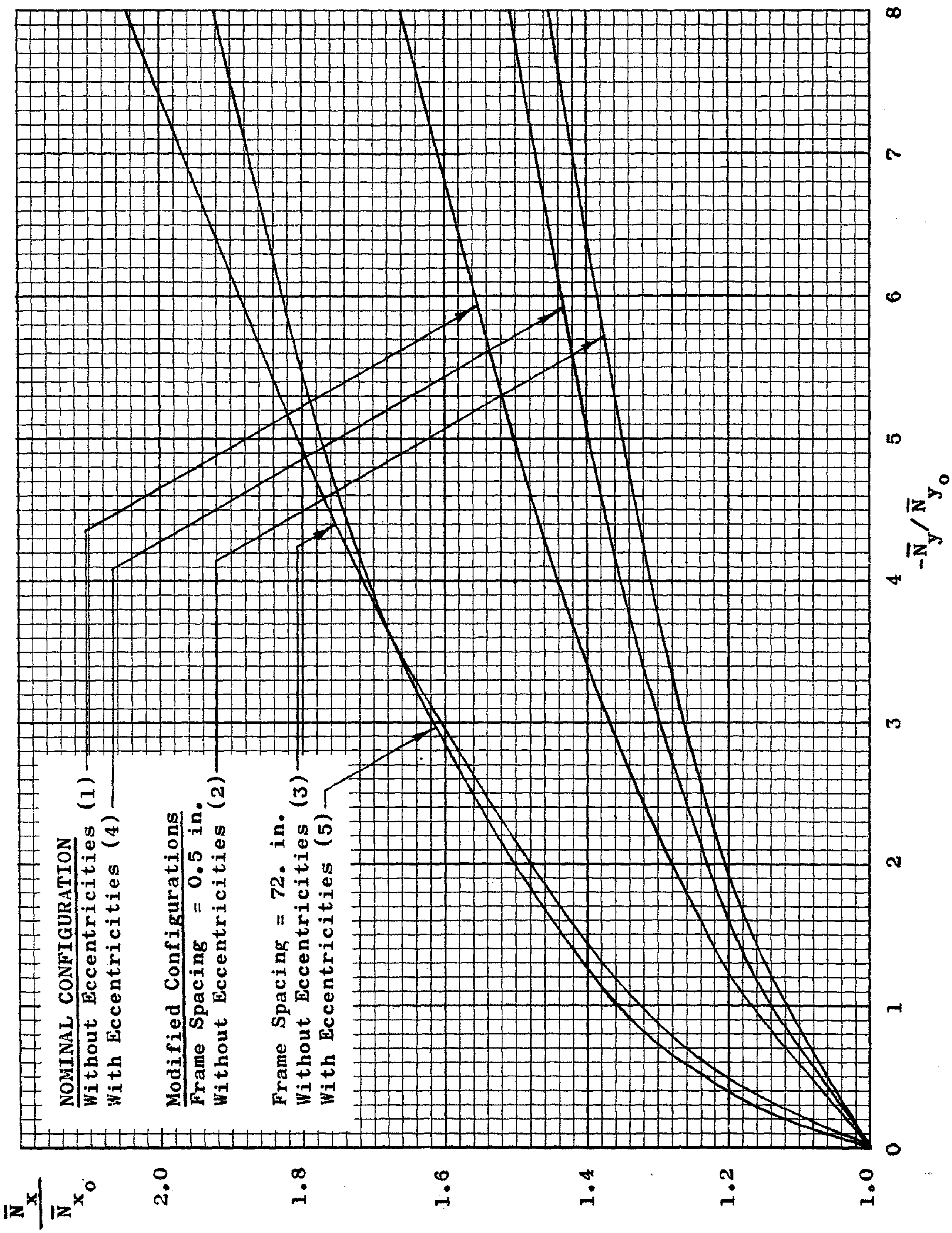

Figure 3 - Stability Interaction Results for Combined Axial Compression and Internal Radial Pressure

SECTION 4

DESIGN CURVES

4.1 FIRST APPROXIMATIONS

From the contents of the foregoing sections, it can be readily appreciated that rather complex computations are required before one can plot accurate interaction curves for eccentrically stiffened circular cylinders. Therefore, in the early stages of design, it might often be helpful to make crude estimates of the true interaction behavior. For cases of

(a) Axial compression plus radial crushing pressure
(b) Axial compression plus overall bending
(c) Axial compression plus in-surface shear $(\overline{N}_{xy})$
(d) Overall bending plus in-surface shear $(\overline{N}_{xy})$

the simple straight-line plot of Figure 4 could be used for such purposes. The parametric studies of SECTION 3 and reference 8 tend to indicate that this crude approximation would give conservative estimates for combinations (a) and (b), respectively. In addition, the limited test data of reference 13 indicate similar conservatism for combination (d).

4.2 IMPROVED APPROXIMATIONS

In order to obtain improved accuracy over that afforded by Figure 4, one could make use of standard dimensional analysis concepts to arrive at approximate interaction curves for eccentrically stiffened cylinders. To understand the approach which might be taken in this connection, a discussion is given here for the particular case of axial compression acting in combination with radial crushing pressure. For this case, one can apply the theoretical solution of Block et al. [1]. The major difficulty encountered in attempting to develop related interaction curves arises out of the large number of independent variables required for the description of particular configurations. From equations (2-10) and (2-11), it can be seen that, for cylinders made of a single isotropic material, the interaction behavior is a function of the following:

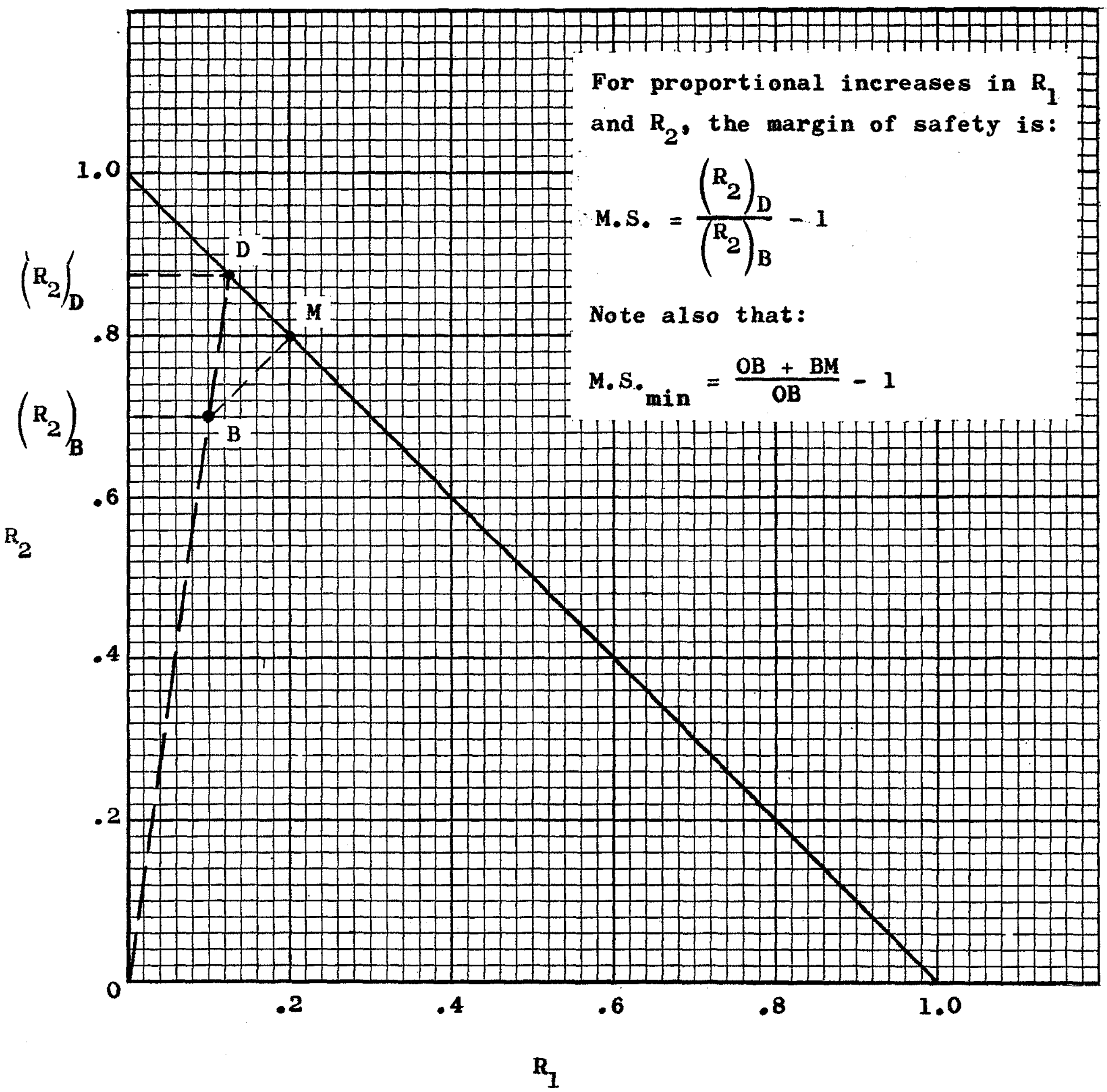

Figure 4 - First-Approximation Interaction Design Curve

$\bar{N}_x$	(A_s/d)	R
$\bar{N}_y$	(A_r/ℓ)	a
E	$\left(I_{o_s}/d\right)$	t
G	$\left(I_{o_r}/\ell\right)$	$\bar{z}_s$
μ	(J_s/d)	$\bar{z}_r$
	(J_r/ℓ)	

As a first step toward practical simplification of the inherent difficulties, it is reasonable to take $\mu = .30$ for all cases. One can then employ the relationship

$$G = \frac{E}{2(1+\mu)} \tag{4-1}$$

to express G in terms of E. Furthermore, for many structures, the torsional constants J_s and J_r will not play very significant roles. Therefore, in the interest of simplicity, one might choose to set both of these values equal to zero. In fact, this is probably a prudent practice even where simplification is not an objective.

As a result of the several foregoing considerations, the array of variables involved in the interaction analysis reduces to the following:

$\bar{N}_x$	(A_s/d)	a
$\bar{N}_y$	(A_r/ℓ)	t
E	$\left(I_{o_s}/d\right)$	$\bar{z}_s$
R	$\left(I_{o_r}/\ell\right)$	$\bar{z}_r$

For added convenience, note that the ratios $\left(I_{o_s}/d\right)$ and $\left(I_{o_r}/\ell\right)$ can be rewritten as

$$\frac{I_{o_s}}{d} = \frac{\bar{I}_s}{d} + \frac{A_s}{d}\left(\bar{z}_s\right)^2$$

$$\frac{I_{o_r}}{\ell} = \frac{\bar{I}_r}{\ell} + \frac{A_r}{\ell}\left(\bar{z}_r\right)^2 \qquad (4\text{-}2)$$

where,

$\bar{I}_s$ = Centroidal moment of inertia of single stringer (no basic cylindrical skin included).

$\bar{I}_r$ = Centroidal moment of inertia of single ring (no basic cylindrical skin included).

Because of these relationships, the above list of relevant variables can be revised to the following:

$\bar{N}_x$	(A_s/d)	a
$\bar{N}_y$	(A_r/ℓ)	t
E	$(\bar{I}_s/d)$	$\bar{z}_s$
R	$(\bar{I}_r/\ell)$	$\bar{z}_r$

At this point it becomes helpful to apply the Buckingham Pi Theorem [14] which constitutes the primary dimensional analysis concept of interest to the present discussion. For this purpose it is first noted that the above reduced listing includes 12 variables which only involve the two basic dimensions of force and length (pounds and inches, for example). From the Buckingham Pi Theorem, it therefore follows that the interaction behavior can be expressed in terms of 10 (= 12-2) dimensionless ratios which may be chosen as

$$\left(\frac{\bar{N}_x}{ER}\right) \qquad \left(\frac{A_s}{dR}\right) \qquad \left(\frac{R}{t}\right)$$

$$\left(\frac{\bar{N}_y}{ER}\right) \qquad \left(\frac{A_r}{\ell R}\right) \qquad \left(\frac{\bar{z}_s}{R}\right)$$

$$\left(\frac{a}{R}\right) \qquad \left(\frac{\bar{I}_s}{dR^3}\right) \qquad \left(\frac{\bar{z}_r}{R}\right)$$

$$\left(\frac{\bar{I}_r}{\ell R^3}\right)$$

Thus the critical value for $(\bar{N}_y/ER)$ can be expressed as follows:

$$\left(\frac{\bar{N}_y}{ER}\right) = f_1 \left[\frac{\bar{N}_x}{ER}, \frac{a}{R}, \frac{A_s}{dR}, \frac{A_r}{\ell R}, \frac{\bar{I}_s}{dR^3}, \frac{\bar{I}_r}{\ell R^3}, \frac{R}{t}, \frac{\bar{z}_s}{R}, \frac{\bar{z}_r}{R}\right] \tag{4-3}$$

One can then proceed by introducing the quantities $\bar{N}_{x_o}$ and $\bar{N}_{y_o}$ where

$\bar{N}_{x_o}$ = Critical value of axial compressive loading when acting alone.

$\bar{N}_{y_o}$ = Critical value of circumferential compressive loading when acting alone.

Simple algebraic operations then lead to the following result:

$$\left(\frac{\bar{N}_y}{\bar{N}_{y_o}}\right) = f_2 \left[\frac{\bar{N}_x}{\bar{N}_{x_o}}, \frac{a}{R}, \frac{A_s}{dR}, \frac{A_r}{\ell R}, \frac{\bar{I}_s}{dR^3}, \frac{\bar{I}_r}{\ell R^3}, \frac{R}{t}, \frac{\bar{z}_s}{R}, \frac{\bar{z}_r}{R}\right] \tag{4-4}$$

Note that the number of relevant variables is still unwieldy for the plotting of design curves. However, for selected values of the ratios

$$\left(\frac{R}{t}\right) ; \left(\frac{\bar{I}_s}{dR^3}\right) ; \left(\frac{\bar{I}_r}{\ell R^3}\right) ; \left(\frac{a}{R}\right)$$

it should be possible to select reasonable, practical magnitudes for the remaining ratios. Approximate interaction curves could then be plotted which would provide more realistic preliminary estimates than can be obtained from Figure 4. Such procedures were followed in the development of the curves given in Figure 5. These plots are furnished here only as examples of what might be accomplished along these lines. Within the scope of the investigation covered by this volume, it did not prove possible to refine this approach to a sufficient degree to obtain practical curves for direct application to actual structures. Some of the values selected in the generation of these curves resulted in rather unrealistic situations. Nevertheless, the plots do demonstrate an approach which might be further developed in the future. Such development should include further study to arrive at reasonable practical ratio values. In addition, additional consideration might be given to alternative formats for the data presentation.

$R/t = 500$ $\qquad \frac{a}{R} = 2.0$ $\qquad \frac{\bar{I}_s}{dR^3} = 1 \times 10^{-6}$

Stringers Outside, Frames Inside

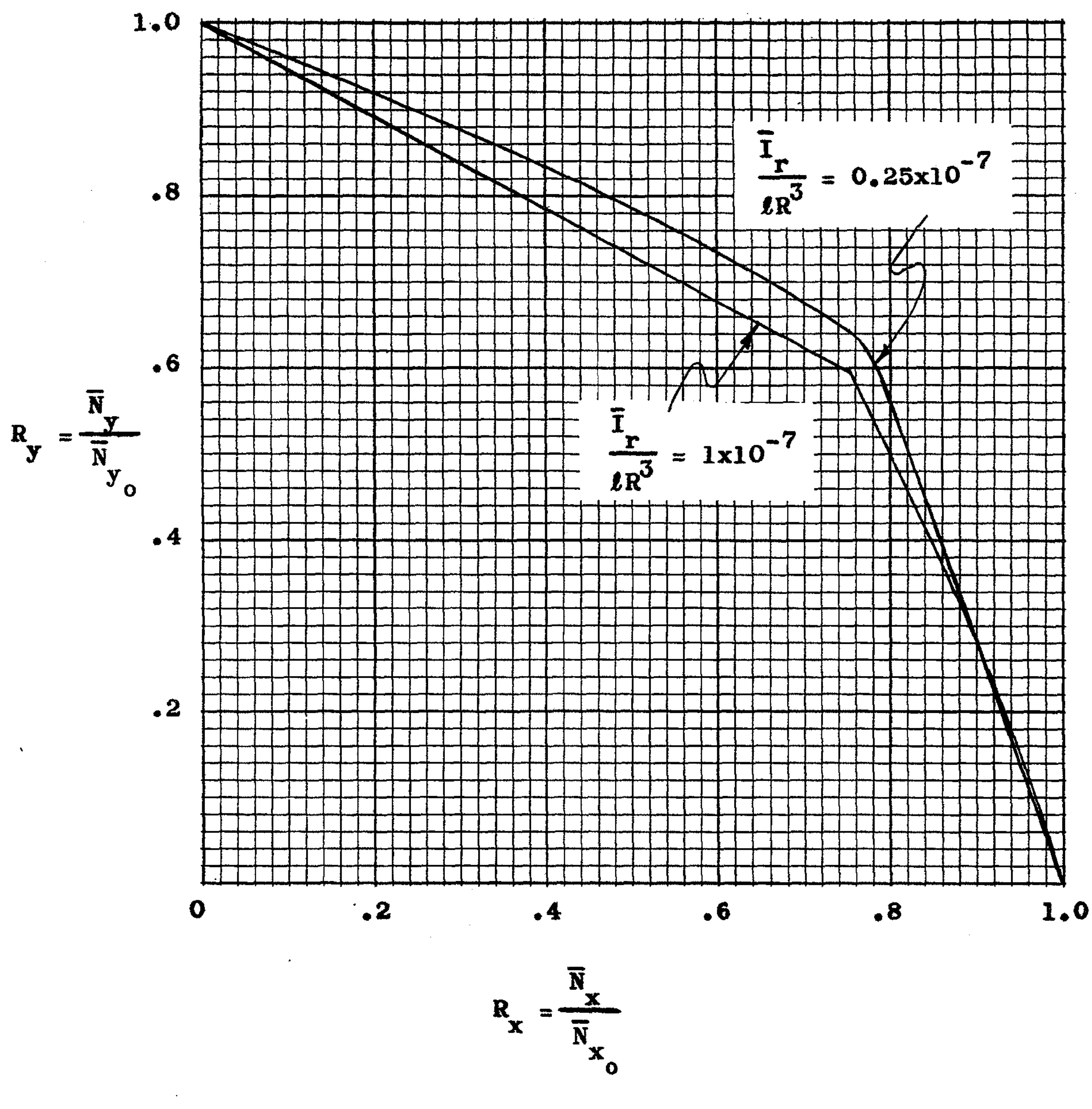

Figure 5(a) - Sample Improved-Approximation Interaction Design Curves for Combined Axial Compression and External Radial Pressure

$R/t = 500$ $\quad \frac{a}{R} = 2.0$ $\quad \frac{\bar{I}_s}{dR^3} = 6 \times 10^{-6}$

Stringers Outside, Frames Inside

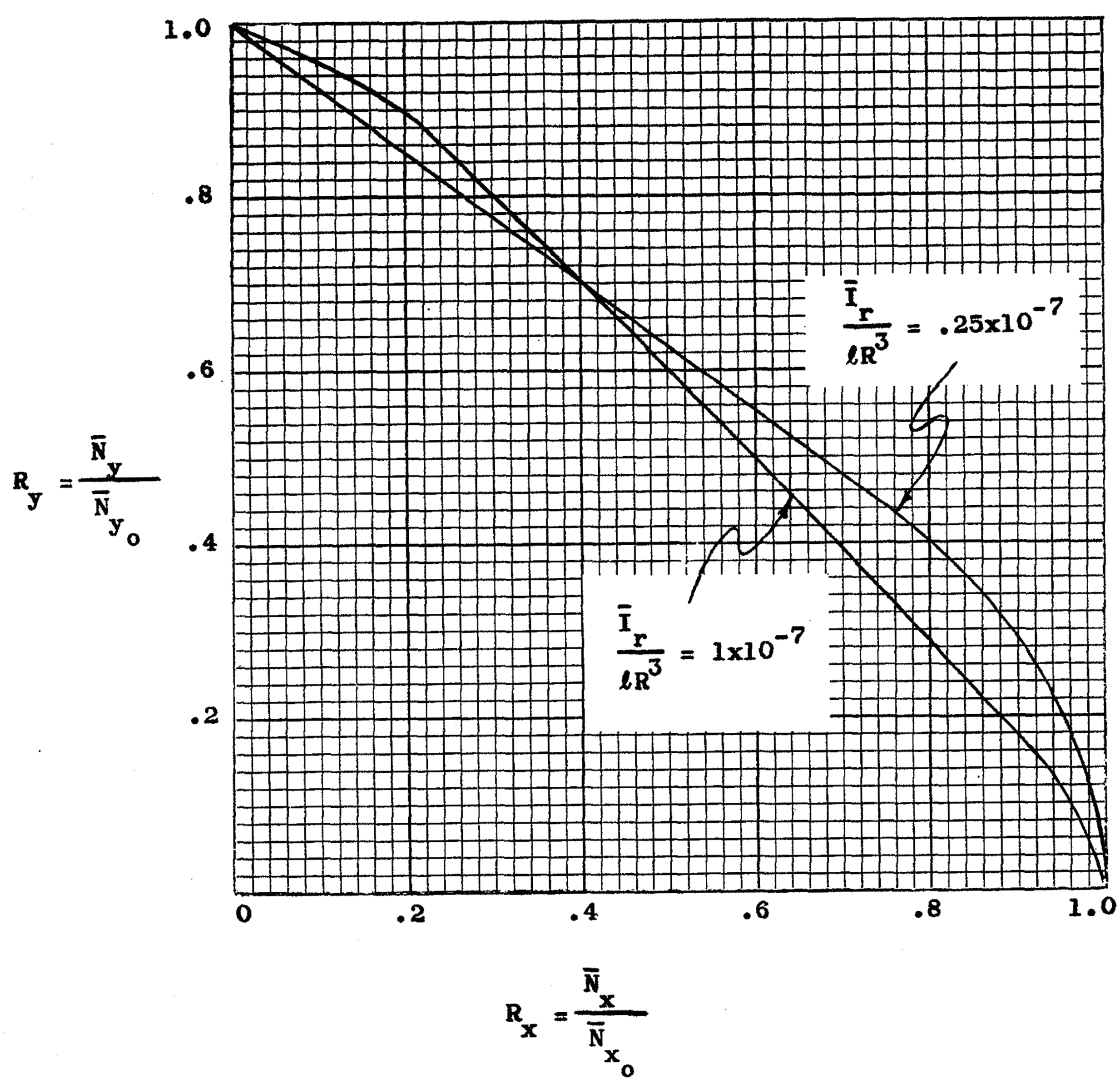

Figure 5(b) - Sample Improved - Approximation Interaction Design Curves for Combined Axial Compression and External Radial Pressure

$R/t = 1000$ $\frac{a}{R} = 2.0$ $\frac{\bar{I}_s}{dR^3} = .4x10^{-6}$

Stringers Outside, Frames Inside

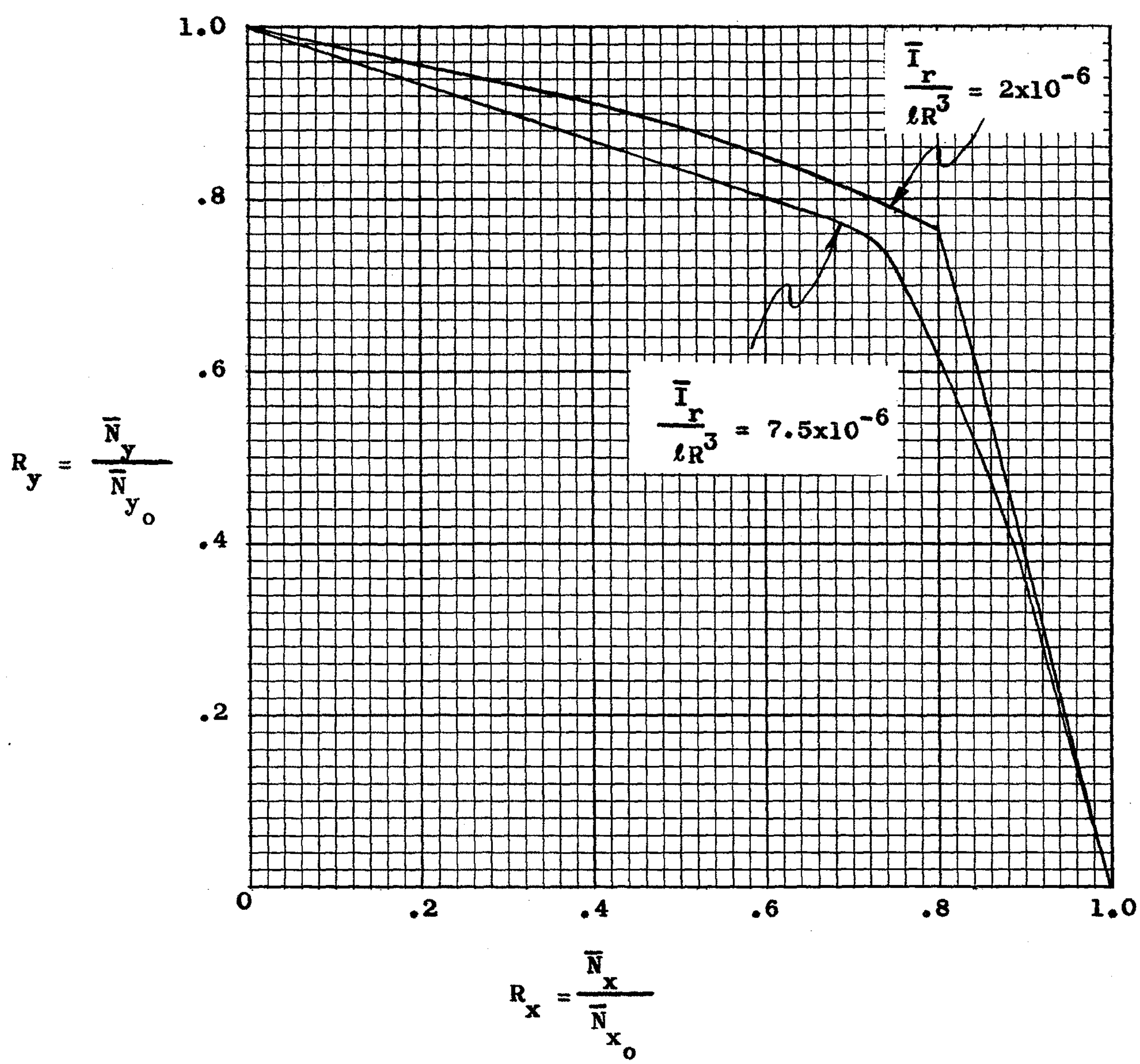

Figure 5(c) - Sample Improved-Approximation Interaction Design Curves for Combined Axial Compression and External Radial Pressure

$R/t = 1000$ $\frac{a}{R} = 2.0$ $\frac{\bar{I}_s}{dR^3} = 2\times10^{-6}$

Stringers Outside, Frames Inside

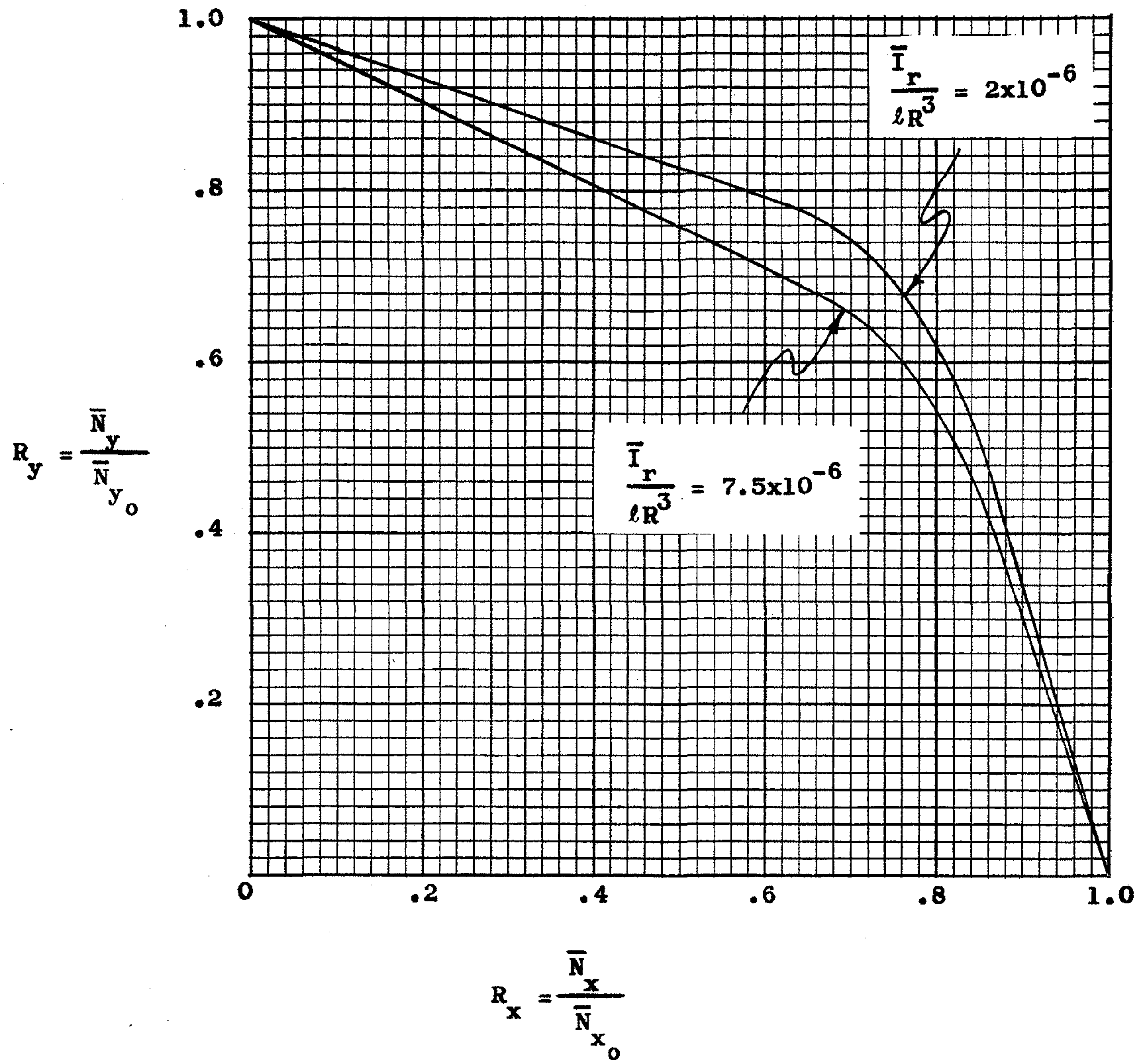

Figure 5(d) - Sample Improved-Approximation Interaction Design Curves for Combined Axial Compression and External Radial Pressure

R/t = 5000 $\frac{a}{R} = 2.0$ $\frac{\bar{I}_s}{dR^3} = 1.5x10^{-8}$

Stringers Outside, Frames Inside

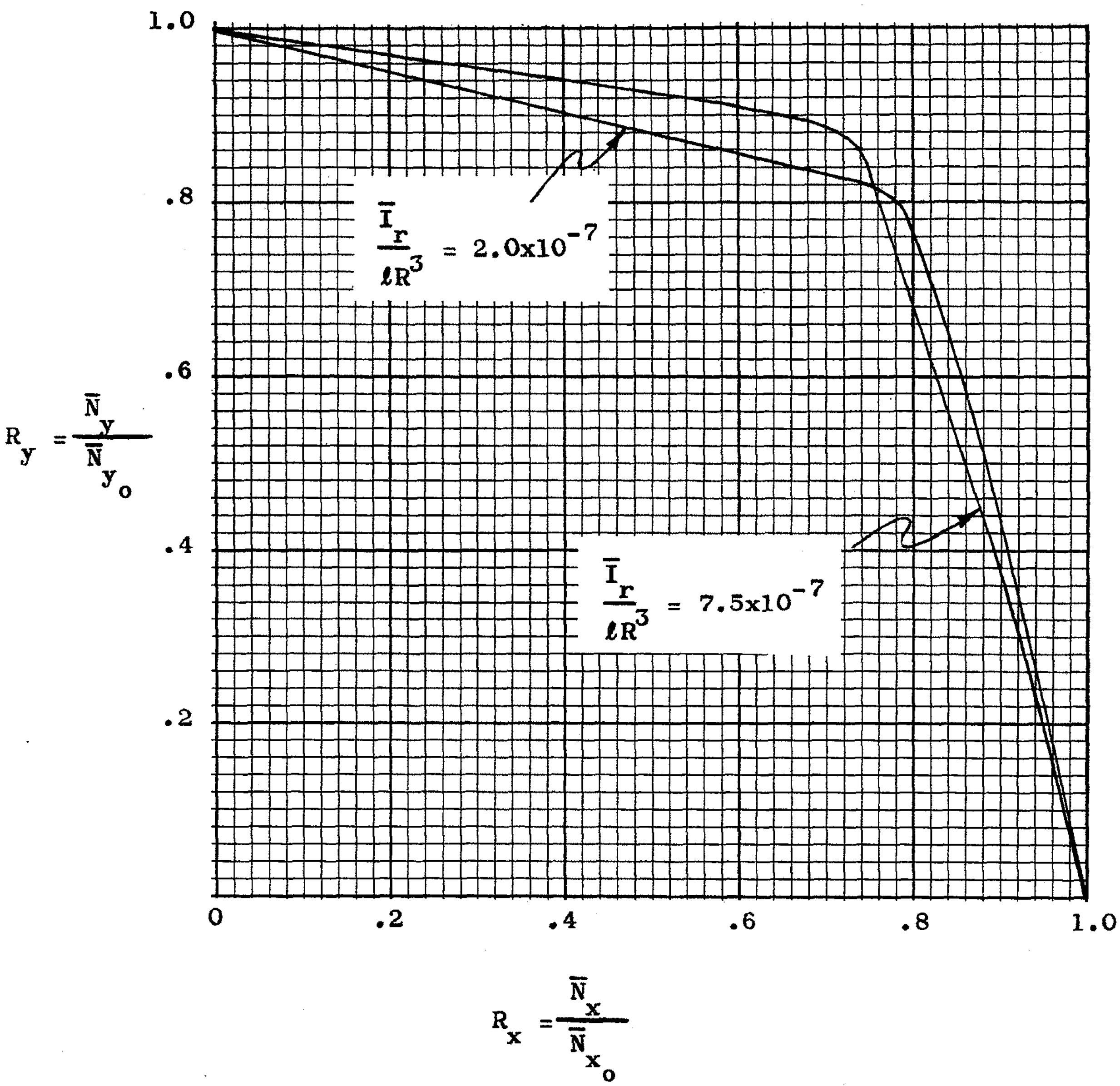

<u>Figure 5(e) - Sample Improved-Approximation Interaction Design Curves for Combined Axial Compression and External Radial Pressure</u>

$R/t = 5000$ $\frac{a}{R} = 2.0$ $\frac{\overline{I}_s}{dR^3} = 7.5\text{x}10^{-8}$

Stringers Outside, Frames Inside

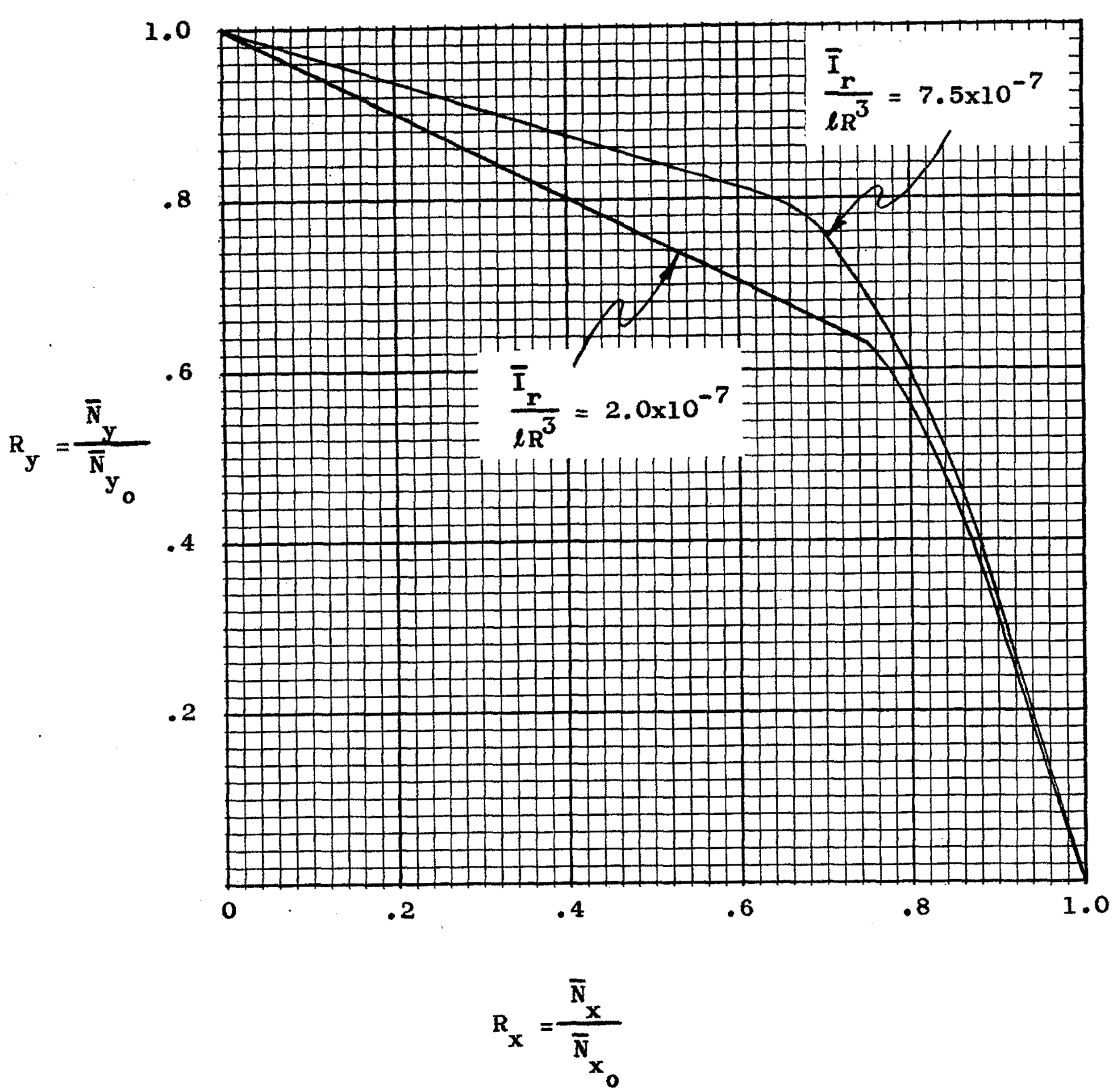

Figure 5(f) - Sample Improved-Approximation Interaction Design Curves for Combined Axial Compression and External Radial Pressure

SECTION 5

DIGITAL COMPUTER PROGRAM

This section presents the essential features of General Dynamics Convair digital computer program numbered 3962. This program was developed to implement the theoretical solution developed by Block, et al. [1] for the buckling of eccentrically stiffened circular cylinders subjected to axial load and/or radial pressure. The program allows for the input of $\overline{N}_y$ or $\overline{N}_x$ (+ = compression, - = tension) along with the m and n values to be screened.

m = Number of axial half-waves in buckle pattern.

n = Number of circumferential full-waves in buckle pattern.

The $\overline{N}_x$ (or $\overline{N}_y$) value is computed for each m-n combination specified by the user. The lowermost computed $\overline{N}_x$ (or $\overline{N}_y$) is always retained throughout the process and the final overall minimum value is printed out as the critical loading. Judgement must be exercised by the user to insure that the actual minimum-strength buckle pattern does not lie outside the range of m and n values screened. The input format is shown in Figure 6. Symbols are listed in Table III. A detailed, card-by-card description of the input follows below. Runs may be stacked.

CARD TYPE 1: One card per run.

Enter PROBLEM IDENTIFICATION (any alphanumeric characters) in columns 1-72.

CARD TYPE 2: One card per run.

Enter NCASES (number of cases) as right adjusted integer in columns 1-5.

Enter PRNTOP (printout option) as right adjusted integer in columns 6-10. If PRNTOP = 0 (or blank), only output corresponding to minimum $\overline{N}$ are printed. If PRNTOP = 1 (or $\neq 0$), all output associated with each m and n combination screened are printed including the A_{ij} values used in equation (2-10).

FORTRAN CODING AND DATA FORM

PROBLEM: ANGLEY SØLUTIØN | AWO | EWO
CODER: S. FØSSUM | EXT. | DATE | PAGE 1 | OF 1

	1–10	11–20	21–30	31–40	41–50	51–60	61–70	71–80
1	PRØBLEM IDENTIFICATIØN							
2	NCASES PRNTØP							
3	CASENØ LØADIN	MINM	MAXM	DELTAM	MINN	MAXN	DELTAN	N̄Y ØR N̄X
4	RADIUS	LENGTH	STRSP	FRAMSP				
5	EX	EY	DX	DY	GXY	DXY		
6	PRIMMX	PRIMMY	MX	MY				
7	ES	GS	AS	IØS	JS	ZBARS		
8	ER	GR	AR	IØR	JR	ZBARR		

FORM AD32 (4-58) CONVAIR | ASTRONAUTICS

Figure 6 - Input Format - Program 3962

CARD TYPE 3: One card per case.

Enter CASENO (case number) as right adjusted alphanumeric characters in columns 1-5.

Enter LOADIN (loading condition) in columns 6-10 with the symbols:

COMBY if $\overline{N}_y$ value input on CARD TYPE 3.

COMBX if $\overline{N}_x$ value input on CARD TYPE 3.

Enter MINM (minimum m value for screening) in columns 11-20 (E10.5). MINM > 0.

Enter MAXM (maximum m value for screening) in columns 21-30 (E10.5).

Enter DELTAM (Δm) in columns 31-40 (E10.5).

Enter MINN (minimum n value for screening) in columns 41-50 (E10.5). MINN > 0 for COMBX. MINN ≥ 0 for COMBY.

Enter MAXN (maximum n value for screening) in columns 51-60 (E10.5).

Enter DELTAN (Δn) in columns 61-70 (E10.5).

Enter $\overline{\text{NY}}$ ($\overline{N}_y$) or $\overline{\text{NX}}$ ($\overline{N}_x$) in columns 71-80 (E10.5). When $\overline{\text{NY}}$ is input, the program computes the critical $\overline{\text{NX}}$ value. When $\overline{\text{NX}}$ is input, the program computes the critical $\overline{\text{NY}}$ value. ($\overline{\text{NX}}$ and $\overline{\text{NY}}$ are positive for compression and negative for tension).

CARD TYPE 4: One card per case.

Enter RADIUS (R, cylinder radius measured to mid-surface of skin, in.) in columns 1-10 (E10.5).

Enter LENGTH (a, overall length of cylinder, in) in columns 11-20 (E10.5).

Enter STRSP (d, stringer spacing, in.) in columns 21-30 (E10.5).

Enter FRAMSP (ℓ, frame spacing, in.) in columns 31-40 (E10.5).

CARD TYPE 5: One card per case.

Enter EX (E_x, lbs/in) in columns 1-10 (E10.5).

Enter EY (E_y, lbs/in) in columns 11-20 (E10.5).

Enter DX (D_x, lb-in) in columns 21-30 (E10.5).

Enter DY (D_y, lb-in) in columns 31-40 (E10.5).

Enter GXY (G_{xy}, lbs/in) in columns 41-50 (E10.5).

Enter DXY (D_{xy}, lb-in) in columns 51-60 (E10.5).

CARD TYPE 6: One card per case.

Enter PRIMMX (μ_x') in columns 1-10 (E10.5).

Enter PRIMMY (μ_y') in columns 11-20 (E10.5).

Enter MX (μ_x) in columns 21-30 (E10.5).

Enter MY (μ_y) in columns 31-40 (E10.5).

CARD TYPE 7: One card per case.

Enter ES (E_s, psi) in columns 1-10 (E10.5).

Enter GS (G_s, psi) in columns 11-20 (E10.5).

Enter AS (A_s, in^2) in columns 21-30 (E10.5).

Enter IOS (I_{o_s}, in^4) in columns 31-40 (E10.5).

Enter JS (J_s, in^4) in columns 41-50 (E10.5).

Enter ZBARS ($\bar{z}_s$, in) in columns 51-60 (E10.5); positive for external stringers; negative for internal stringers.

CARD TYPE 8: One card per case.

Enter ER (E_r, psi) in columns 1-10 (E10.5).

Enter GR (G_r, psi) in columns 11-20 (E10.5).

Enter AR (A_r, in^2) in columns 21-30 (E10.5).

Enter IOR (I_{o_r}, in^4) in columns 31-40 (E10.5).

Enter JR (J_r, in^4) in columns 41-50 (E10.5).

Enter ZBARR ($\bar{z}_r$, in) in columns 51-60 (E10.5); positive for external rings; negative for internal rings.

A sample input coding form is shown in Figure 7. A sample output listing is given in Figure 8. A basic flow diagram is presented in Figure 9 and a Fortran listing of the program is shown in Table IV.

TABLE III - Program 3962 Notation

PROGRAM NOTATION	REPORT NOTATION	DESCRIPTION
AR	A_r	Cross-sectional area of circumferential stiffener, in^2 .
AS	A_s	Cross-sectional area of longitudinal stiffener, in^2.
CASENO	-	Case number.
COMBX	-	Indicates $\bar{N}_x$ value input, solve for $\bar{N}_y$.
COMBY	-	Indicates $\bar{N}_y$ value input, solve for $\bar{N}_x$.
D	-	See STRSP.
DX	D_x	Bending stiffness of skin in longitudinal direction, lb-in.
DY	D_y	Bending stiffness of skin in circumferential direction, lb-in.
DXY	D_{xy}	Twisting stiffness of skin, lb-in.
DELTAM	Δm	Value by which m is incremented.
DELTAN	Δn	Value by which n is incremented.
ER	E_r	Young's modulus for circumferential stiffener, psi.
ES	E_s	Young's modulus for longitudinal stiffener, psi.
EX	E_x	Extensional stiffness of skin in longitudinal direction, lbs/in.
EY	E_y	Extensional stiffness of skin in circumferential direction, lbs/in.

TABLE III - Program 3962 Notation
(Continued)

PROGRAM NOTATION	REPORT NOTATION	DESCRIPTION
ERARL	$E_r A_r/\ell$	
FRAMSP	ℓ	Frame spacing, in.
FMPIA	$m\pi/a$	
FMXMY	$1-\mu_x'\mu_y'$	
GMXMY	$1-\mu_x\mu_y$	
GR	G_r	Shear modulus for circumferential stiffener, psi.
GS	G_s	Shear modulus for longitudinal stiffener, psi.
GXY	G_{xy}	In-plane shear stiffness of skin panel, lbs/in.
IOR	I_{o_r}	Moment of inertia of circumferential stiffener cross-section about middle surface of skin, in^4.
IOS	I_{o_s}	Moment of inertia of longitudinal stiffener cross-section about middle surface of skin, in^4.
JR	J_r	Torsional constant for circumferential stiffener, in^4.
JS	J_s	Torsional constant for longitudinal stiffener, in^4.
LENGTH	a	Length of stiffened cylinder, in.
LOADIN	-	Option describing input loading: COMBY or COMBX.
MAXM	-	Maximum value of m used.

TABLE III - Program 3962 Notation
(Continued)

PROGRAM NOTATION	REPORT NOTATION	DESCRIPTION
MINM	-	Minimum value of m used.
MAXN	-	Maximum value of n used.
MINN	-	Minimum value of n used.
MX	μ_x	Poisson's ratio for bending of skin in longitudinal direction.
MY	μ_y	Poisson's ratio for bending of skin in circumferential direction.
NBAR	$\overline{N}$	$\overline{N}_x$ or $\overline{N}_y$ (+ in compression) lbs/in.
NCASES	-	Number of cases.
NOP	-	NOP = 1 used for COMBY NOP = 2 used for COMBX
NXORNY	$\overline{N}_x$ or $\overline{N}_y$	$\overline{N}_x$ or $\overline{N}_y$ input, lbs/in.
PRIMMX	μ_x'	Poisson's ratio for extension of skin in longitudinal direction.
PRIMMY	μ_y'	Poisson's ratio for extension of skin in circumferential direction.
PRNTOP	-	Printout option. If PRINTOP = 0 (or blank), prints only output associated with minimum value of $\overline{N}$ calculated. If PRNTOP$\neq$0, prints output for all combinations of m and n values screened.
PROBID	-	Problem identification.
RADIUS	R	Radius of cylinder, measured to mid-surface of skin, in.

TABLE III - Program 3962 Notation
(Continued)

PROGRAM NOTATION	REPORT NOTATION	DESCRIPTION
STOREM	-	m for minimum $\bar{N}$.
STOREN	-	n for minimum $\bar{N}$.
STRSP	d	Stringer spacing, in.
TEMP	-	Relative minimum $\bar{N}$.
ZBARR	$\bar{z}_r$	Distance from middle surface of skin to centroid of circumferential stiffener, in., positive if stiffener is outside.
ZBARS	$\bar{z}_s$	Distance from middle surface of skin to centroid of longitudinal stiffener in., positive if stiffener is outside.

FORTRAN CODING AND DATA FORM

PROBLEM	LANGLEY SØLUTIØN			AWO	EWO
CODER	L.S. FØSSUM	EXT.	DATE	PAGE 1	OF 1

```
        SAMPLE PRØBLEM
    1CØMBY   1.0      25.0      1.0                25.0       1.0       2.0
  38.6      72.0       2.48      6.0
   1.5 +06   2.0 +06 250.0     300.0       2.0 +05 200.0
    .25       .35       .25       .35
  30.0 +06  12.0 +06    .02       .005      .004  +.05
  25.0 +06  10.0 +06    .04       .010      .006  -.10
```

FIGURE 7 - Sample Input Data - Program 3962

CASE NO.	MIN M	MAX M	DELTA M	MIN N	MAX N	DELTA N
1	1.0000E 00	2.5000E 01	1.0000E 00	-0.	2.5000E 01	1.0000E 00

CYLINDER RADIUS	OVERALL LENGTH	STRINGER SPACING	FRAME SPACING		N BAR Y
3.8600E 01	7.2000E 01	2.4800E 00	6.0000E 00		2.0000E 00

E SUB X	E SUB Y	D SUB X	D SUB Y	G SUB XY	D SUB XY
1.5000E 06	2.0000E 06	2.5000E 02	3.0000E 02	2.0000E 05	2.0000E 02

MU PRIME SUB X	MU PRIME SUB Y	MU SUB X	MU SUB Y
2.5000E-01	3.5000E-01	2.5000E-01	3.5000E-01

E SUB S	G SUB S	A SUB S	I SUB OS	J SUB S	Z BAR SUB S
3.0000E 07	1.2000E 07	2.0000E-02	5.0000E-03	4.0000E-03	5.0000E-02

E SUB R	G SUB R	A SUB R	I SUB OR	J SUB R	Z BAR SUB R
2.5000E 07	1.0000E 07	4.0000E-02	1.0000E-02	6.0000E-03	-1.0000E-01

CRITICAL COMBINED LOAD VALUES

NUMBER OF LONGITUDINAL HALF WAVES	NUMBER OF CIRCUMFERENTIAL HALF WAVES	AXIAL LOAD BAR SUB X LBS PER IN	HOOP LOAD BAR SUB Y LBS PER IN
4.0000E 00	1.4000E 01	7.8588E 03	2.0000E 00
3.0000E 00	1.4000E 01	8.0546E 03	2.0000E 00
5.0000E 00	1.4000E 01	8.3383E 03	2.0000E 00
4.0000E 00	1.2000E 01	8.1912E 03	2.0000E 00
4.0000E 00	1.6000E 01	8.3470E 03	2.0000E 00

Figure 8 - Sample Output Listing - Program 3962

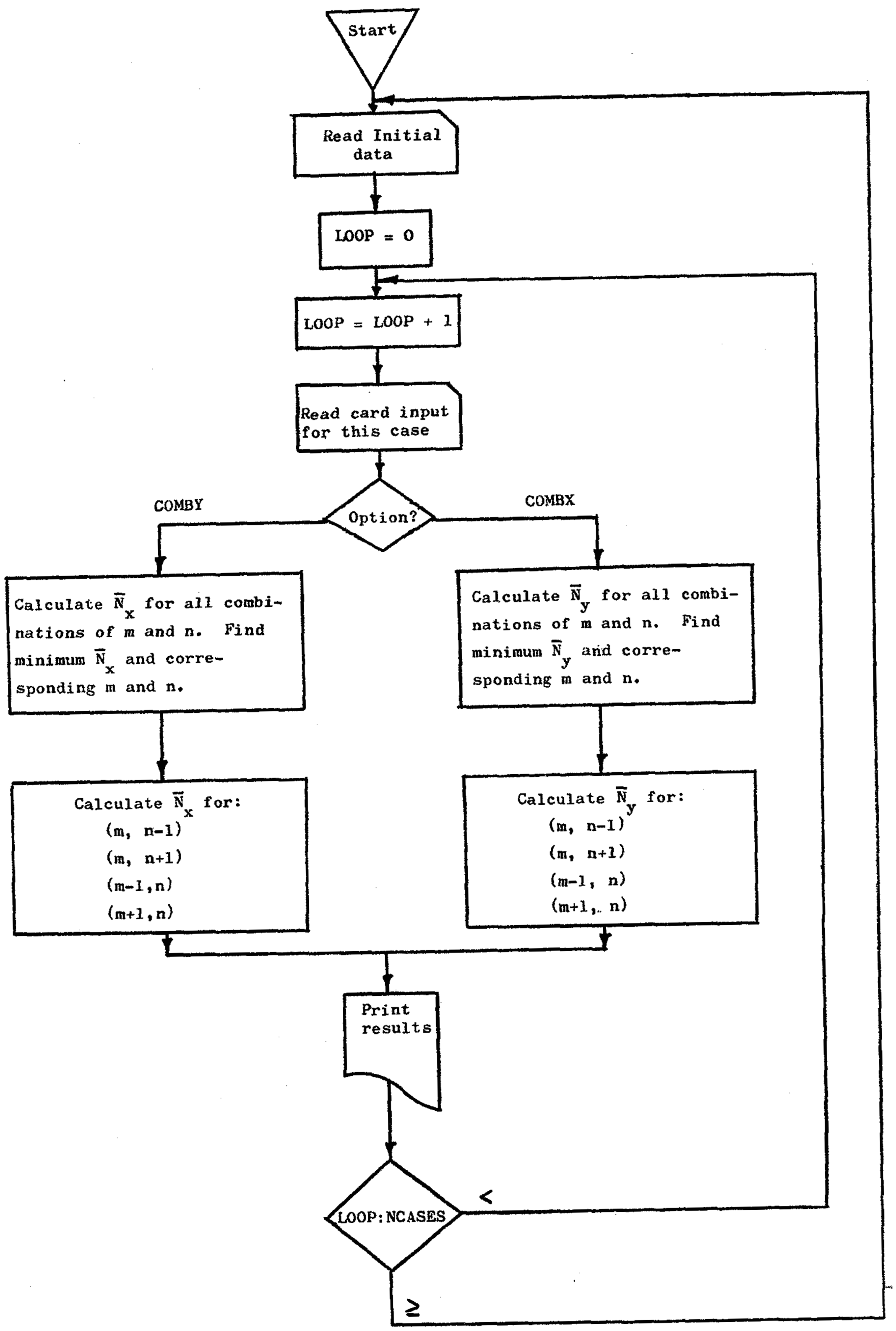

Figure 9 - Flow Diagram - Program 3962

TABLE IV - Fortran Listing - Program 3962

```
$IBFTC MAIN    LIST
      COMMON /INPT/    CASENO,LOADIN,MINM,MAXM,DELTAM,MINN,MAXN,DELTAN,
     1                 RADIUS,LENGTH,STRSP,FRAMSP,EX,EY,DX,DY,GXY,DXY,
     2                 PRIMMX,PRIMMY,MX,MY,ES,GS,AS,IOS,JS,ZBARS,ER,GR,
     3                 AR,IOR,JR,ZBARR,NOP,PI,PRNTOP,NXORNY
      DIMENSION PROBID(12)
      REAL MINM,MAXM,MINN,MAXN,LENGTH,MX,MY,IOS,JS,IOR,JR,NBAR,NXORNY
      INTEGER COMBX,COMBY
      DATA COMBX,COMBY /5HCOMBX,5HCOMBY/
      DATA   PI /3.1415926/
  100 READ (5,101) PROBID
  101 FORMAT (12A6)
      WRITE (6,201) PROBID
  201 FORMAT (1H1,20(/),58X,16HLANGLEY SOLUTION 10(/),30X,12A6)
      READ (5,301) NCASES,PRNTOP
  301 FORMAT (I5,F5.0)
      DO 1000 N=1,NCASES
      CALL INPUT
      IF (PRNTOP.EQ.0.) GO TO 310
      WRITE (6,305) CASENO
  305 FORMAT (1H1,50X,28HINTERMEDIATE VALUES FOR CASE,A5)
  310 NOP=0
      IF (LOADIN.EQ.COMBY) NOP=1
      IF (LOADIN.EQ.COMBX) NOP=2
      IF (NOP.NE.0) GO TO 400
      WRITE (6,350) CASENO
  350 FORMAT (/// 87X,31HOPTION GIVEN INCORRECTLY, CASE A3, 8H DELETED)
      GO TO 1000
  400 CALL EQUATN
  500 CALL FINAL
  600 CALL OUTPUT
 1000 CONTINUE
      GO TO 100
      END
$IBFTC NBAR    LIST
      REAL FUNCTION NBAR(EX,FMXMY,ES,AS,D,FMPIA,GXY,FNR,PRIMMY,R,ZBARS,
     1                  EY,ERARL,ZBARR,DX,IOS,DXY,GS,JS,GR,JR,L,DY,ER,
     2                  IOR,N,NOP,M,PRNTOP,NXORNY,MY,GMXMY)
      REAL IOS,JS,JR,L,IOR,N,M,NXORNY
      REAL MY
      A11 = (EX / FMXMY + ES*AS/D) * FMPIA**2  +  GXY*FNR**2
      A12 = (PRIMMY*EX/FMXMY + GXY) * FMPIA * FNR
      A13 = (1./R)*(PRIMMY*EX/FMXMY)*FMPIA + ES*AS/D*ZBARS*FMPIA**3
      A22 = GXY*FMPIA**2 + (EY/FMXMY + ERARL) * FNR**2
      A23 = (1./R) * (EY/FMXMY + ERARL) * FNR + ERARL*ZBARR*FNR**3
      A33 = (DX/GMXMY + ES*IOS/D)*FMPIA**4 + (2.*MY*DX/GMXMY
     1      + 2.*DXY + GS*JS/D + GR*JR/L) * FMPIA**2 * FNR**2
     2      + (DY/GMXMY + ER*IOR/L)*FNR**4 + (1./R**2)*(EY/FMXMY
     3      + ERARL)  +  (2.*ERARL*ZBARR*(N**2/R**3) )
      GO TO (1000,2000), NOP
C
```

TABLE IV - Fortran Listing - Program 3962
(Continued)

```
C      NOP=1
 1000 DIV = FMPIA**2
      SUB = FNR**2 * NXORNY
      GO TO 4000
C
C      NOP=2
 2000 DIV = FNR**2
      SUB = FMPIA**2 * NXORNY
C
 4000 NBAR = (A33 + ( ((A12*A23)-(A13*A22))/((A11*A22)-A12**2))*A13
     1       + ((((A12*A13)-(A11*A23))/((A11*A22)-A12**2) )*A23 ) - SUB)
     2       / DIV
      IF (PRNTOP.EQ.0.) RETURN
      WRITE (6,6000) M,N,NBAR,A11,A12,A13,A22,A23,A33
 6000 FORMAT (/// 11X,5HM    =,1PE11.3,28X,5HN    =,1PE11.3,28X,6HN BAR=,
     1        E16.9 // 11X,5HA11 =,1PE17.9,22X,5HA12 =,1PE17.9, 22X,
     2       5HA13 =,1PE17.9, // 11X,5HA22 =,1PE17.9,22X,5HA23 =,1PE17.9,
     3        22X,5HA33 =,1PE17.9)
      RETURN
      END
$IBFTC INPUT   LIST
      SUBROUTINE INPUT
      COMMON /INPT/   CASENO,LOADIN,MINM,MAXM,DELTAM,MINN,MAXN,DELTAN,
     1                RADIUS,LENGTH,STRSP,FRAMSP,EX,EY,DX,DY,GXY,DXY,
     2                PRIMMX,PRIMMY,MX,MY,ES,GS,AS,IOS,JS,ZBARS,ER,GR,
     3                AR,IOR,JR,ZBARR,NOP,PI,PRNTOP,NXORNY
      REAL MINM,MAXM,MINN,MAXN,LENGTH,MX,MY,IOS,JS,IOR,JR,NBAR,NXORNY
C
C      SUBROUTINE TO READ CARD INPUT FOR EACH CASE.
      READ (5,101) CASENO,LOADIN,MINM,MAXM,DELTAM,MINN,MAXN,DELTAN
     *             ,NXORNY
  101 FORMAT (2A5,7E10.5)
      READ (5,201) RADIUS,LENGTH,STRSP,FRAMSP
  201 FORMAT (4E10.5)
      READ (5,301) EX,EY,DX,DY,GXY,DXY
  301 FORMAT (6E10.5)
      READ (5,201) PRIMMX,PRIMMY,MX,MY
      READ (5,301) ES,GS,AS,IOS,JS,ZBARS
      READ (5,301) ER,GR,AR,IOR,JR,ZBARR
      RETURN
      END
$IBFTC EQUATN  LIST
      SUBROUTINE EQUATN
      COMMON /INPT/   CASENO,LOADIN,MINM,MAXM,DELTAM,MINN,MAXN,DELTAN,
     1                RADIUS,LENGTH,STRSP,FRAMSP,EX,EY,DX,DY,GXY,DXY,
     2                PRIMMX,PRIMMY,MX,MY,ES,GS,AS,IOS,JS,ZBARS,ER,GR,
     3                AR,IOR,JR,ZBARR,NOP,PI,PRNTOP,NXORNY
      COMMON /INTER/ FMXMY,ERARL,TEMP,STOREM,STOREN,GMXMY
      COMMON /RENAME/ A,D,L,R
      REAL MINM,MAXM,MINN,MAXN,LENGTH,MX,MY,IOS,JS,IOR,JR,NBAR
      REAL L,M,N,NBARX,NBARY,NXORNY
```

TABLE IV - Fortran Listing - Program 3962
(Continued)

```
      R=RADIUS
      A=LENGTH
      D=STRSP
      L=FRAMSP
      FMXMY = 1.-PRIMMX*PRIMMY
      GMXMY = 1.-MX*MY
      ERARL = ER*AR/L
      ICNT=0
      N=MINN-DELTAN
  100 N=N+DELTAN
      IF (N.GT.MAXN) GO TO 6000
      FNR = N/R
      M=MINM-DELTAM
  200 M=M+DELTAM
      ICNT=ICNT+1
      IF (M.GT.MAXM) GO TO 5000
      FMPIA = M*PI/A
      GO TO (1000,2000), NOP
C
C     NOP=1  SOLVE FOR N BAR X
 1000 NBARX = NBAR(EX,FMXMY,ES,AS,D,FMPIA,GXY,FNR,PRIMMY,R,ZBARS,EY,
     1              ERARL,ZBARR,DX,IOS,DXY,GS,JS,GR,JR,L,DY,ER,IOR,N,NOP,
     2              M,PRNTOP,NXORNY,MY,GMXMY)
      IF (ICNT.NE.1) GO TO 1100
      TEMP=NBARX
      STOREM=M
      STOREN=N
      GO TO 4000
 1100 IF (NBARX.GE.TEMP) GO TO 4000
      TEMP=NBARX
      STOREM=M
      STOREN=N
      GO TO 4000
C
C     NOP=2  SOLVE FOR N BAR Y
 2000 NBARY = NBAR(EX,FMXMY,ES,AS,D,FMPIA,GXY,FNR,PRIMMY,R,ZBARS,EY,
     1              ERARL,ZBARR,DX,IOS,DXY,GS,JS,GR,JR,L,DY,ER,IOR,N,NOP,
     2              M,PRNTOP,NXORNY,MY,GMXMY)
      IF (ICNT.NE.1) GO TO 2100
      TEMP=NBARY
      STOREM=M
      STOREN=N
      GO TO 4000
 2100 IF (NBARY.GE.TEMP) GO TO 4000
      TEMP=NBARY
      STOREM=M
      STOREN=N
C
 4000 GO TO 200
 5000 GO TO 100
 6000 RETURN
```

TABLE IV - Fortran Listing - Program 3962 (Continued)

```
      END
$IBFTC FINAL   LIST
      SUBROUTINE FINAL
      COMMON /INPT/    CASENO,LOADIN,MINM,MAXM,DELTAM,MINN,MAXN,DELTAN,
     1                 RADIUS,LENGTH,STRSP,FRAMSP,EX,EY,DX,DY,GXY,DXY,
     2                 PRIMMX,PRIMMY,MX,MY,ES,GS,AS,IOS,JS,ZBARS,ER,GR,
     3                 AR,IOR,JR,ZBARR,NOP,PI,PRNTOP,NXORNY
      COMMON /OUT/     X(5),Y(5),VALUE(5)
      COMMON /INTER/ FMXMY,ERARL,TEMP,STOREM,STOREN,GMXMY
      COMMON /RENAME/ A,D,L,R
      DIMENSION FN(5)
      REAL MINM,MAXM,MINN,MAXN,LENGTH,MX,MY,IOS,JS,IOR,JR,NBAR,M,N
     1    ,NXORNY
      VALUE(1)=TEMP
      X(1)=STOREM
      Y(1)=2.0*STOREN
      FN(1)=STOREN
      X(2)=X(1)-1.0
      X(3)=X(1)+1.
      X(4)=X(1)
      X(5)=X(1)
      Y(2)=Y(1)
      FN(2)=FN(1)
      Y(3)=Y(1)
      FN(3)=FN(1)
      Y(4)=Y(1)-2.0
      FN(4)=FN(1)-1.0
      Y(5)=Y(1)+2.0
      FN(5)=FN(1)+1.0
      DO 500  I=2,5
      FMPIA = X(I)*PI/A
      FNR = FN(I)/R
      N = FN(I)
      M=X(I)
      VALUE(I) = NBAR(EX,FMXMY,ES,AS,D,FMPIA,GXY,FNR,PRIMMY,R,ZBARS,EY,
     1                 ERARL,ZBARR,DX,IOS,DXY,GS,JS,GR,JR,L,DY,ER,IOR,N,
     2                 NOP,M,PRNTOP,NXORNY,MY,GMXMY)
  500 CONTINUE
      RETURN
      END
$IBFTC OUTPUT  LIST
      SUBROUTINE OUTPUT
      COMMON /INPT/    CASENO,LOADIN,MINM,MAXM,DELTAM,MINN,MAXN,DELTAN,
     1                 RADIUS,LENGTH,STRSP,FRAMSP,EX,EY,DX,DY,GXY,DXY,
     2                 PRIMMX,PRIMMY,MX,MY,ES,GS,AS,IOS,JS,ZBARS,ER,GR,
     3                 AR,IOR,JR,ZBARR,NOP,PI,PRNTOP,NXORNY
      COMMON /OUT/     X(5),Y(5),VALUE(5)
      REAL MINM,MAXM,MINN,MAXN,LENGTH,MX,MY,IOS,JS,IOR,JR,NBAR,NXORNY
      WRITE (6,100) CASENO,MINM,MAXM,DELTAM,MINN,MAXN,DELTAN
  100 FORMAT (1H1,1X,8HCASE NO.,9X,5HMIN M,16X,5HMAX M,14X,7HDELTA M,
     1       14X,5HMIN N,15X,5HMAX N,14X,7HDELTA N // 1X,A6,1P6E20.4 )
```

TABLE IV - Fortran Listing - Program 3962
(Continued)

```
      GO TO (200,250), NOP
  200 WRITE (6,201) RADIUS,LENGTH,STRSP,FRAMSP,NXORNY
  201 FORMAT (/// 18X,8HCYLINDER,12X,7HOVERALL,13X,8HSTRINGER,13X,
     1       5HFRAME / 19X,6HRADIUS,14X,6HLENGTH,14X,7HSPACING,12X,
     2       7HSPACING,34X,7HN BAR Y // 7X,1P4E20.4,1PE40.4)
      GO TO 299
  250 WRITE (6,251) RADIUS,LENGTH,STRSP,FRAMSP,NXORNY
  251 FORMAT (/// 18X,8HCYLINDER,12X,7HOVERALL,13X,8HSTRINGER,13X,
     1       5HFRAME / 19X,6HRADIUS,14X,6HLENGTH,14X,7HSPACING,12X,
     2       7HSPACING,34X,7HN BAR X // 7X,1P4E20.4,1PE40.4)
  299 WRITE (6,300) EX,EY,DX,DY,GXY,DXY
  300 FORMAT (/// 18X,7HE SUB X,13X,7HE SUB Y,13X,7HD SUB X,13X,
     1       7HD SUB Y,13X,8HG SUB XY,12X,8HD SUB XY // 7X,1P6E20.4 )
      WRITE (6,400) PRIMMX,PRIMMY,MX,MY
  400 FORMAT (/// 18X,8HMU PRIME,12X,8HMU PRIME / 19X,5HSUB X,15X,
     1       5HSUB Y,14X,8HMU SUB X,12X,8HMU SUB Y // 7X,1P6E20.4 )
      WRITE (6,500) ES,GS,AS,IOS,JS,ZBARS
  500 FORMAT (/// 119X,5HZ BAR / 18X,7HE SUB S,13X,7HG SUB S,13X,
     1       7HA SUB S,13X,8HI SUB OS,12X,7HJ SUB S,14X,5HSUB S //
     2       7X,1P6E20.4 )
      WRITE (6,600) ER,GR,AR,IOR,JR,ZBARR
  600 FORMAT (/// 119X,5HZ BAR / 18X,7HE SUB R,13X,7HG SUB R,13X,
     1       7HA SUB R,13X,8HI SUB OR,12X,7HJ SUB R,14X,5HSUB R //
     2       7X,1P6E20.4 )
      WRITE (6,700)
  700 FORMAT (6(/),51X,29HCRITICAL COMBINED LOAD VALUES ///
     *         12X, 9HNUMBER OF, 24X,
     1         9HNUMBER OF,24X,10HAXIAL LOAD,23X,9HHOOP LOAD / 11X,
     2         12HLONGITUDINAL,19X,15HCIRCUMFERENTIAL,21X,9HBAR SUB X,
     3         24X,9HBAR SUB Y / 12X,10HHALF WAVES,23X,10HHALF WAVES,
     4         23X,10HLBS PER IN,23X,10HLBS PER IN // )
      GO TO (1000,2000),NOP
 1000 WRITE (6,1001) (X(I),Y(I),VALUE(I),NXORNY,I=1,5)
 1001 FORMAT (1X,1PE21.4,1P3E33.4//(1X,1PE21.4,1P3E33.4))
      RETURN
 2000 WRITE (6,1001) (X(I),Y(I),NXORNY,VALUE(I),I=1,5)
 3000 RETURN
      END
```

SECTION 6

REFERENCES

1. Block, D. L., Card, M. F., and Mikulas, M. M., Jr., "Buckling of Eccentrically Stiffened Orthotropic Cylinders," NASA TN D-2960, August 1965.
2. Dharmarajan, S. N. and Wilson, P. E., "Theoretical Verification and Extension of Langley Buckling Equations for Circular Cylinders Having Eccentric Orthotropic Stiffening," Contract NAS8-11181, General Dynamics Convair Division Memo AS-D-1033, 28 February 1967.
3. Smith, G. W. and Spier, E. E., "The Stability of Eccentrically Stiffened Circular Cylinders, Volume I - General," Contract NAS8-11181, General Dynamics Convair Division Report No. GDC-DDG-67-006, 20 June 1967.
4. Smith, G. W. and Spier, E. E., "The Stability of Eccentrically Stiffened Circular Cylinders, Volume V - Effects of Initial Imperfections; Axial Compression and Pure Bending," Contract NAS8-11181, General Dynamics Convair Division Report No. GDC-DDG-67-006, 20 June 1967.
5. Duncan, W. J., "Galerkin's Method in Mechanics and Differential Equations," Air Ministry Aeronautical Research Committee Reports and Memoranda No. 1798, 3 August 1937.
6. Lakshmikantham, C., Gerard, G., and Milligan, R., "General Instability of Orthotropically Stiffened Cylinders, Part II, Bending and Combined Compression and Bending," Air Force Flight Dynamics Laboratory Technical Report AFFDL TR 65 161, Part II, August 1965.
7. Hedgepeth, J. M. and Hall, D. B., "Stability of Stiffened Cylinders," AIAA Journal, Vol. 3, No. 12, December 1965.
8. Block, D. L., "Buckling of Eccentrically Stiffened Orthotropic Cylinders Under Pure Bending," NASA TN D-3351, March 1966.

SECTION 6

REFERENCES
(Continued)

9. Flügge, W., "Die Stabilität der Kreiszylinderschale," Ingenieur-Archiv, Vol. 3, 1932, pp. 463-506.

10. Flügge, W., Stresses in Shells, Springer-Verlag, Berlin, 1962.

11. Timoshenko, S., Theory of Elastic Stability, McGraw-Hill Book Company, Inc., New York, N. Y., 1932, pp 463-467.

12. Seide, P. and Weingarten, V. I., "On the Buckling of Circular Cylindrical Shells Under Pure Bending," Trans. of the ASME, Journal of Applied Mechanics, March 1961.

13. Anon., "Some Investigations of the General Instability of Stiffened Metal Cylinders, VII - Stiffened Metal Cylinders Subjected to Combined Bending and Torsion," NACA Technical Note No. 911, November 1943.

14. Murphy, C. E., Similitude in Engineering, The Ronald Press Company, New York, 1950.